Université de Montréal

Extension of Wu-Peters Bounds to Catmull-Clark and 4-8 Subdivision

par

Zhe Wu

Département d'informatique et de recherche opérationnelle

Faculté des arts et des sciences

Mémoire présenté à la faculté des études supérieures

en vue de l'obtention du grade de

Maître ès sciences (M.Sc.)

en informatique

Mars 2010

Université de Montréal

Faculté des études supérieures

Ce mémoire de maîtrise intitulé

Extension of Wu-Peters Bounds to Catmull-Clark and 4-8 Subdivision

présenté par

Zhe Wu

a été évalué par un jury composé des personnes suivantes :

Pierre Poulin
président-rapporteur

Neil Stewart
directeur de recherche

Victor Ostromoukhov
membre du jury

Sommaire

La méthode de subdivision Catmull-Clark ainsi que la méthode de subdivision Loop sont des normes industrielles de facto. D'autre part, la méthode de subdivision 4-8 est bien adaptée à la subdivision adaptative, parce que cette méthode augmente le nombre de faces ou de sommets par seulement un facteur de 2 à chaque raffinement. Cela promet d'être plus pratique pour atteindre un niveau donné de précision.

Dans ce mémoire, nous présenterons une méthode permettant de paramétrer des surfaces de subdivision de la méthode Catmull-Clark et de la méthode 4-8. Par conséquent, de nombreux algorithmes mis au point pour des surfaces paramétriques pourrant être appliqués aux surfaces de subdivision Catmull-Clark et aux surfaces de subdivision 4-8. En particulier, nous pouvons calculer des bornes garanties et réalistes sur les patches, un peu comme les bornes correspondantes données par Wu-Peters [24] pour la méthode de subdivision Loop.

Mots clefs:
surface de subdivision, matrice de subdivision locale, patches de surface, paramétrisation.

Abstract

The Catmull-Clark and Loop methods are de facto industry standards. On the other hand, the 4-8 subdivision method is well suited for adaptive subdivision, because this method increases the number of faces or vertices by only a factor of 2 at each step. It is therefore more convenient when trying to achieve a given practical level of precision.

In this thesis we will introduce a method to parametrize the subdivision surfaces of Catmull-Clark and 4-8 subdivision. As a consequence, many algorithms developed for parametric surfaces will be able to be applied to Catmull-Clark and 4-8 subdivision surfaces. In particular, we can produce bounds on surface patches which are both guaranteed and realistic, similar to the bounds given by Wu-Peters [24] for the Loop method.

Keywords:
subdivision surface, local subdivision matrix, surface patch, parametrization.

Contents

List of Figures

Acknowledgment

I am pleased to have had the company of all the friendly people who did also their graduate studies in the computer graphics laboratory at the University of Montreal. I would like to thank Jianghao Chang, Di Jiang, François Duranleau, Luc Leblanc, Marie-Élise Cordeau, Yann Rousseau, Frédéric Rozon and Simon Clavet. Of all these people, I owe special thanks to Di Jiang, because without our intensive discussions, this thesis would not be what it is.

I am also pleased to have had the best teachers during my graduate studies. I would also like to thank Victor Ostromoukhov and Pierre Poulin for their good advices and education courses. But above all, I must thank my research director Neil Stewart. With Neil, I always felt that I was supported to end up with a superb working environment in the laboratory.

Finally, I thank my wife and my parents for their support.

Chapter 1

Introduction

1.1 Background

The publication of the papers by Catmull and Clark [7] and Doo and Sabin [11] in 1978 marked the beginning of subdivision for surface modeling. A subdivision surface is a method of representing a smooth surface via the specification of a coarse polyhedral mesh and a set of rules to refine it.

The limit subdivision surface is generally produced iteratively using a given refinement scheme, but most of the limiting subdivision surfaces can also be evaluated directly in terms of a set of *eigenbasis* functions which depend only on the subdivision scheme [21]. Alternatively, a simpler approach, akin to [17], can approximate the subdivision surface's basis functions.

Subdivision is becoming increasingly popular as a surface representation in computer graphics applications. For animation and simulation, subdivision surfaces fill the gap between polyhedral and spline modeling. Keeping closed seams and tangency between multiple NURBS patches becomes difficult in places where multiple joints exert influence over edges of these multiple surfaces [3]. With subdivision surfaces, we can use a single polygon mesh to define a complex model: there is no need to piece individual patches together.

1.2 The Idea of Subdivision

The basic idea of subdivision is to define a smooth curve or surface as the limit of a sequence of successive refinements. This idea can be traced to G. de Rham [9] who used

"corner cutting" recursively to obtain smooth curves. In 1974, Chaikin [8] introduced a special case of the corner cutting algorithm. Chaikin's algorithm became popular and is often used to illustrate the basic idea of subdivision methods. Chaikin's algorithm applies to curves, rather than to surfaces, but it illustrates clearly [2, Sec. 1.1] the idea of subdivision. We start with a polygon made up of four segments:

1. Two intermediate points are introduced on each segment by taking a weighted average of the corner points, using weights $\left(\frac{1}{4}, \frac{3}{4}\right)$ and $\left(\frac{3}{4}, \frac{1}{4}\right)$, respectively. Connecting these new points produces a polygon with eight segments and eight corners.

2. Previous points are dropped from the polygon.

3. Repeating this process, we will have a polygon with 16 segments and 16 corners, 32 segments and 32 corners, etc. In the limit, the polygon will converge towards a smooth limit curve.

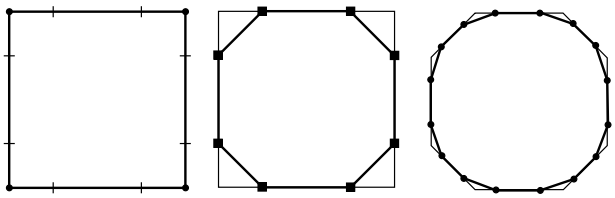

Figure 1.1: Two steps of Chaikin's algorithm [2, Sec. 1.1].

So we can consider subdivision as a repeated refinement process.

1.3 Classification of Subdivision Schemes

Subdivision schemes are quite varied. Here we just discuss the best known stationary subdivision schemes generating C^1-continuous surfaces on arbitrary meshes [26].

We classify the subdivision schemes according to the criteria frequently used:

1. The type of refinement rule (face split or vertex split [26, Sec. 4.1]).

   (a) Face split: Catmull-Clark, Loop, Modified Butterfly, Kobbelt.

   (b) Vertex split: Doo-Sabin, Midedge, Biquartic.

2. The type of generated mesh (primarily triangular or quadrilateral).

(a) Triangular: Loop, Modified Butterfly.

(b) Quadrilateral: Catmull-Clark, Kobbelt.

(c) General: Doo-Sabin, Midedge, Biquatric.

3. Whether the scheme is intrinsically approximating or interpolating.

(a) Approximating: Loop, Catmull-Clark, Doo-Sabin, Midedge, Biquatric.

(b) Interpolating: Modified Butterfly, Kobbelt.

4. Smoothness of the limit surfaces for regular meshes (C^1, C^2, etc.).

(a) C^1-continuous: Modified Butterfly, Kobbelt, Doo-Sabin, Midedge.

(b) C^2-continuous: Loop, Catmull-Clark, Biquartic.

Here, we find that the 4-8 subdivision scheme is a special kind of subdivision scheme with respect to the above classification. It uses bisection refinement as an elementary refinement operation rather than face or vertex splits and the subdivision surfaces produced by the 4-8 scheme are C^4-continuous except at extraordinary vertices where they are C^1-continuous. In this thesis we focus on the Catmull-Clark and 4-8 subdivision methods.

1.4 Outline of the Thesis

The remainder of the thesis is organized as follows. A short overview of the research area of geometric modeling is given in Chapter 2. The main part of the thesis is contained in Chapter 3 and Chapter 4. A detailed introduction to the Catmull-Clark and 4-8 subdivision schemes is given in Chapter 3. In particular, we make several useful comments about the in-place implementation of methods. In Chapter 4, a method extending Wu-Peters [24] is introduced showing how to parametrize the Catmull-Clark and 4-8 subdivision surfaces in a way that permits accurate approximation of the limit surface. This is the main contribution of the thesis. We conclude and mention promising possibilities for future work in Chapter 5.

Chapter 2

Literature Review

2.1 Geometric Modeling

Geometric modeling has rapidly become a central area of research and development that involves diverse applications. It is important in the traditional fields of engineering, general product design, and computer-aided manufacturing. It is also indispensable in a variety of modern industries: computer vision, robotics, medical imaging, visualization, as well as computer graphics, including computer games and animation for films.

2.1.1 Geometric Representations

There are two major representation schemas that are often used: *Constructive Solid Geometry* (CSG) and *Boundary representation* (B-rep). In CSG a solid is represented as a set-theoretic Boolean representation of primitive solid objects. In B-rep the solid surface is represented explicitly as a quilt of vertices, edges, and faces [14].

Non-Uniform Rational B-splines (NURBS) have become a *de facto* industry standard for the representation, design, and data exchange of geometric information processed by computer. Their excellent mathematical and algorithmic properties, combined with successful industrial applications, have contributed to the enormous popularity of NURBS. This method of representing solids is, like the method of subdivision-surface models, a B-rep representation.

2.1.2 Subdivision-Surface Models

Currently, the most common way to model complex smooth surfaces in the domain of geometric modeling is by using a patchwork of trimmed NURBS (*trimming* simply means that a subset of the domain of the B-spline or NURBS surface is delineated as the part of the surface to be used [2, Sec. 1.1]). One of the reasons why trimmed NURBS continue to be widely used is because they are readily available in existing commercial systems and in the kernels on which they are based [1]. However, they suffer from at least two difficulties [10]:

1. Trimming is expensive and prone to numerical and approximation errors.

2. It is difficult to maintain smoothness, or even approximate smoothness, at the seams of the patchwork.

Subdivision surfaces have the ability to overcome these two problems: they do not require trimming, and smoothness of the model is automatically guaranteed.

As already mentioned, the basic idea of subdivision is a repeated refinement process. In a paper titled *Exact Evaluation of Catmull-Clark Subdivision Surfaces at Arbitrary Parameter Values* by Jos Stam [21], it was however shown that subdivision surfaces can alternatively be evaluated directly without explicitly subdividing. Therefore, many algorithms, such as interference detection, developed for parametric surfaces can be applied to subdivision surfaces. This makes subdivision surfaces an even more attractive tool for free-form surface modeling.

2.2 Evaluation of Subdivision Surfaces

We will now give further details concerning subdivision-surface evaluation. The first evaluation method was introduced by Stam [21]: this method parametrizes the control mesh and the limit surface over a single mesh element (triangle or quadrilateral) to evaluate the surface at an arbitrary parameter value. Another method was introduced by Wu-Peters [24]. It uses the linearity of the subdivision process, and a certain parameterization of the limit surface, centered at each vertex, such that the limit surface is evaluated as the linear combination of the basis functions, weighted by the original control points [2, Sec. 6.5][15].

2.2.1 Stam's Method

Stam's method is based on the fact that subdivision surfaces, such as those generated by Catmull-Clark and Loop subdivisions, can be evaluated in terms of a set of eigenbasis functions which depend only on the subdivision scheme. Further, we can derive analytical expressions for these basis functions [21, 20]. Stam's method can be viewed as a generalization of algorithms that evaluate B-spline surfaces using the explicit definitions of the B-spline nodal functions.

We present an overview of the algorithm for the Catmull-Clark case [21] in order to establish the theoretical foundations of this type of method, and to compare it informally with the Wu-Peters method. Otherwise the method is not used in this thesis. We implemented Stam's method, in order to ensure that all the details were understood. In the following descriptions, several of the figures are taken directly from [21].

We assume that the initial mesh has been subdivided at least once, isolating the extraordinary vertices so that each face is a quadrilateral and contains at most one extraordinary vertex ($n \neq 4$). The surface is viewed as a regular surface made up of ordinary B-spline patches, except near the extraordinary vertex, where there are n patches adjacent to the extraordinary vertex, $n \neq 4$, as illustrated in Figure 2.1:

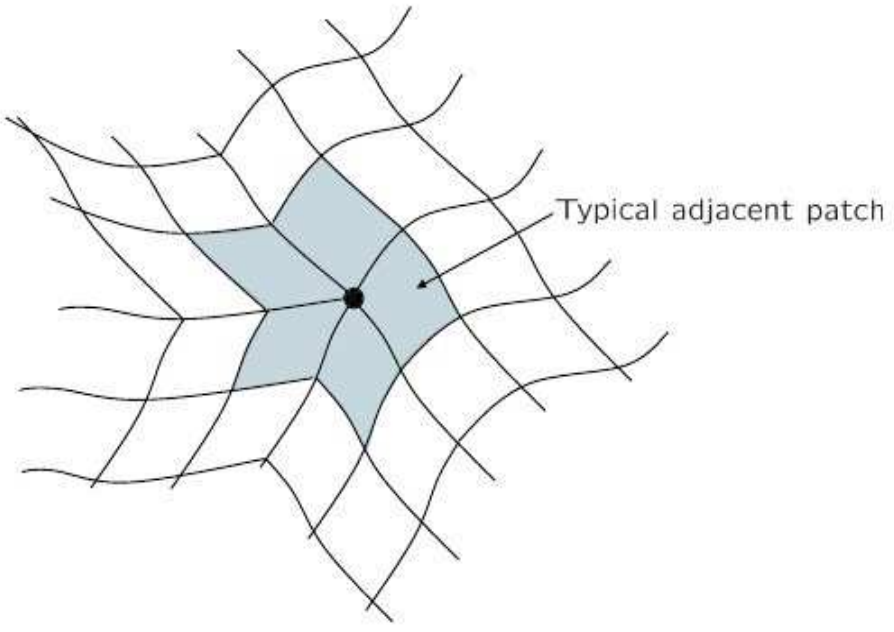

Figure 2.1: Five surface patches around an extraordinary vertex.

The Catmull-Clark subdivision scheme generalizes uniform B-spline knot insertion [6] to meshes of arbitrary topology. For the regular case, Catmull-Clark subdivision is equivalent to midpoint uniform B-spline knot insertion. Therefore, the 16 vertices surrounding a face are the control points of a uniform bi-cubic B-spline patch.

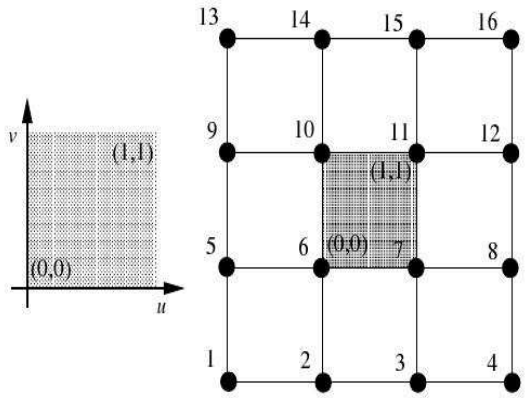

Figure 2.2: A bi-cubic B-spline is defined by 16 control points. The numbers are the ordering of the corresponding B-spline basis functions in the vector $b(u, v)$ defined by Stam.

Because the control vertex structure near an extraordinary vertex is not a rectangular grid, the faces containing extraordinary vertices cannot be evaluated as uniform B-splines. We need to demonstrate how to evaluate a patch corresponding to a face with an extraordinary vertex. Our goal is to find a surface patch $s(u, v)$ defined over the unit square $\Omega = [0, 1] \times [0, 1]$ which can be evaluated directly in terms of the $K = 2n + 8$ vertices that influence the shape of the patch corresponding to the face [21]. We assume that the extraordinary vertex corresponds to $(0, 0)$ and the ordering of the control points is defined as in Figure 2.3.

We define a surface patch around an extraordinary vertex and choose a certain ordering of the control points of the patch, as shown in Figure 2.3. We denote the initial vector of control points by

$$C_0^T = (c_{0,1}, ..., c_{0,K}).$$

Through subdivision we can generate a new set of $M = K + 9$ vertices shown in

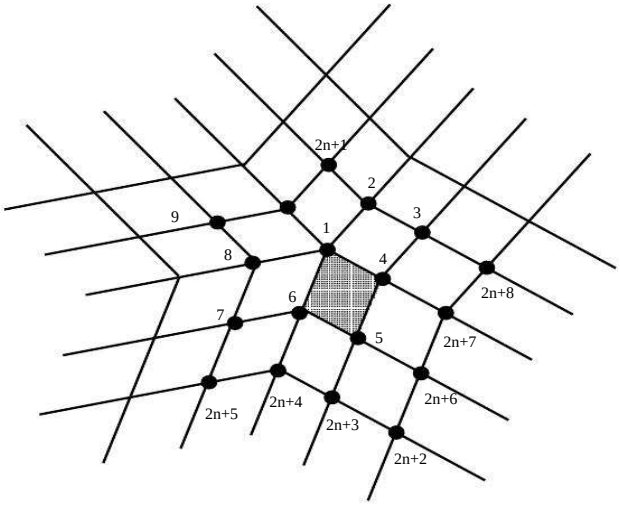

Figure 2.3: Domain for surface patch adjacent to a vertex with valence n= 5.

Figure 2.4 as circles super-imposed on the initial vertices. The initial control points of the surface patch are shown in Figure 2.3. This is what is required to completely define the patch in the dark-shaded area in Figure 2.3. With a $K \times K$ subdivision matrix A, we have:

$$C_1 = AC_0,$$

where A is $K \times K$ subdivision matrix having the form:

$$A = \begin{pmatrix} S & 0 \\ S_{11} & S_{12} \end{pmatrix},$$

and where S is a $(2n+1) \times (2n+1)$ subdivision matrix [13]. The matrices S_{11} and S_{12} are two matrices for regular knot insertion for B-splines. An extra set of vertices is also needed to evaluate the three B-spline patches that are defined using a bigger matrix $\bar{A}$ (see Figure 2.4):

$$\bar{C_\kappa} = \bar{A}A^{\kappa-1}C_0, \quad \kappa > 1,$$

where $\bar{A}$ is a $(2n+17) \times K$ matrix, the matrix A is $K \times K$, and C_0 is $K \times 3$. The value of κ is the number of subdivision steps.

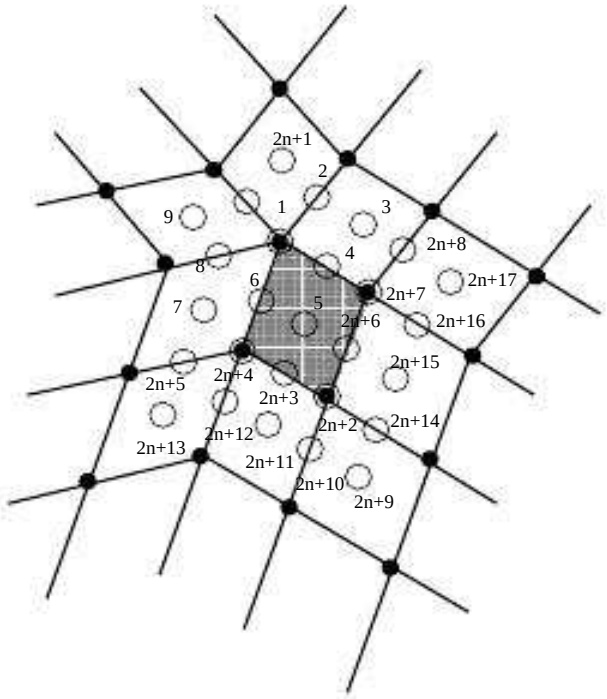

Figure 2.4: Addition of new vertices by applying the Catmull-Clark subdivision rule to the vertices in Figure 2.3.

For each level $\kappa \geq 1$, a subset of the vertices of $\bar{C_\kappa}$ becomes the set of control vertices of three B-spline patches. These control vertices can be defined by selecting 16 control vertices from $\bar{C_\kappa}$ and storing them in three 16×3 matrices:

$$B_{k,\kappa} = P_k \bar{C_\kappa},$$

where P_k is a $16 \times M$ matrix and $k = 1, 2, 3$. Let $b(u, v)$ be the 16×3 vector containing the 16 cubic B-spline basis functions, then the surface patch corresponding to each matrix of control vertices is defined as:

$$s_{k,\kappa}(u, v) = B_{k,\kappa}^T b(u, v) = \bar{C_\kappa^T} P_k^T b(u, v),$$

where $(u, v) \in \Omega, \kappa \geq 1$ and $k = 1, 2, 3$. There is an infinite sequence of uniform B-spline patches defined by the above equations which form our surface $s(u, v)$. This is done by partitioning the unit square Ω into an infinite set of tiles Ω_k^κ, $\kappa \geq 1$, $k = 1, 2, 3$, as shown in Figure 2.6.

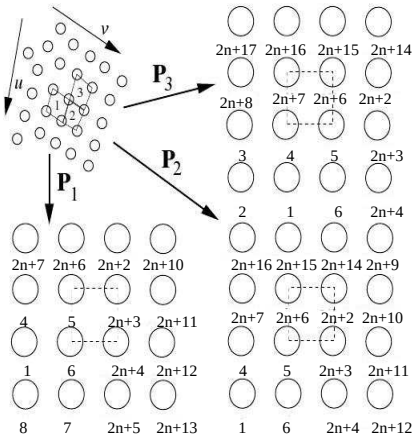

Figure 2.5: Indices of the control vertices of the three bi-cubic B-spline patches.

However, it is very costly to evaluate the surface, since it involves $\kappa-1$ multiplications of the $K \times K$ matrix A. The evaluation can be simplified considerably by computing the eigenstructure of A.

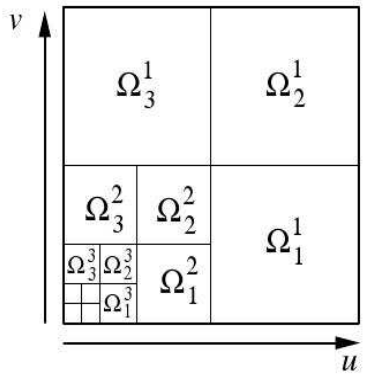

Figure 2.6: Partition of the unit square into an infinite family of tiles.

Eigenstructure

In the Catmull-Clark case, for the $K \times K$ matrix A, there exist K linearly independent eigenvectors and the matrix A can be decomposed as:

$$A = VDV^{-1},$$

by *singular value decomposition*, where D is a diagonal matrix containing the eigenvalues of A, and V is an invertible matrix whose columns are the corresponding eigenvectors.

Therefore, given the singular value decomposition, we can compute $A^{\kappa-1}$ as:

$$A^{\kappa-1} = VD^{\kappa-1}V^{-1} = Vdiag(\lambda_0^{\kappa-1}, \lambda_1^{\kappa-1}, \ldots, \lambda_{K-1}^{\kappa-1})V^{-1}.$$

where κ is the number of multiplications of the matrix A and K is the number of eigenvalues of the matrix A. The evaluation of the surface requires only $O(K^3)$ operations and it is independent of the value of κ.

2.2.2 Wu-Peters Method

The capability of evaluating subdivision surfaces is only one aspect of the Wu-Peters method. The method is mainly used to do safe and efficient interference detection for subdivision surfaces [24] and to measure errors for adaptive subdivision surfaces [25].

Both interference detection for subdivision surfaces and accurate error measures for adaptive subdivision surfaces require safe linear approximations of the limit surfaces. Approximation of the limit surface by the subdivided control polyhedron can be both inaccurate and costly (there is exponential growth of the number of faces). The Wu-Peters method permits us to define a bound on the maximum distance between the limit surface and its linear approximation. The bound can be computed locally and efficiently.

Wu and Peters [24, 25] illustrated their approach with Loop's subdivision scheme [18]. The basic and the most important step of the Wu-Peters method is to define a set of Loop patches. A Loop patch is a piece of the limit surface under Loop subdivision applied to the triangle and its one-ring neighbors. If each of the vertices of the triangles has six neighbors, it is called a *regular* patch. Otherwise, it is irregular. We assume that at most one of the vertices has $n \neq 6$ neighbors. We assume that extraordinary vertices are separated by at least one ordinary vertex. This is always the case after one local subdivision step. The principle of patch design is to ensure that the domains of the Loop patches lie inside the center triangles. This is important because the bounding volume is parametrized over the center triangle. On the other hand, the patch domain should cover the center triangle as much as possible, since a larger gap means a larger overestimate. Having the Loop patches, we can approximate the nodal functions and build local bounding volumes that tightly sandwich the limit surfaces.

These local bounding volumes are created using linear upper and lower bounds on each of the x, y, z components of the limit surfaces. The x, y and z components of the limit surfaces are bounded by forming a linear combination of pre-computed bounds on the nodal functions [2, Sec. 2.2].

In this thesis, we mainly focus on the parametrization of the subdivision surfaces. We extend the Wu-Peters method to the Catmull-Clark and 4-8 subdivision surfaces. Thus, in the following sections we present two important aspects of the Wu-Peters method: finding the nodal functions and parametrization of the Loop patches.

Nodal Functions and Evaluation of Subdivision Surfaces

The so-called *basis functions* in the Wu-Peters method, an inaccurate word in the case of the Loop method, are called *nodal functions*. Given the control patch, the spanning functions of one spatial coordinate of a generalized subdivision surface are called nodal functions. They can be obtained by simply applying the subdivision process, provided it is convergent, until the approximation is satisfactory, to control points that associate the value one with one node and zero with all others [2, Sec. 2.2].

According to the Wu-Peters method, a nodal function ξ_i corresponds to the ith control point of the Loop patches, where $i = 0, \ldots, \mu$ and $\mu + 1$ is the number of control points of one Loop patch. Suppose we have a regular Loop patch and we want to compute the nodal function ξ_0 which is associated with the node v_0 in the (u, v) domain. We set the z component of the control point associated with v_0 equal to one and the z component of all other control points equal to zero. Since the bounding volumes of the limit surfaces are naturally parametrized over the center triangles of the Loop patches, we are only interested in the nodal function's range over the center triangle: 2D parameter domain (see Figure 2.7 where the nodes v_i are denoted simply by i, $i = 0, ..., 11$). Notice that the calculation of the nodal functions of the Wu-Peters method is independent of the type of the Loop patches, that is to say, whether the patch is regular or irregular, we use the same method to find the nodal functions.

Now we can just apply the Loop subdivision scheme to these control points. After seven subdivision steps (we use the same number of subdivision steps as Wu-Peters), we obtain an adequate approximation of the nodal function ξ_0 (see Figure 2.8).

$$s(u, v) = \sum_{i=0}^{\mu} \xi_i(u, v) p_i$$

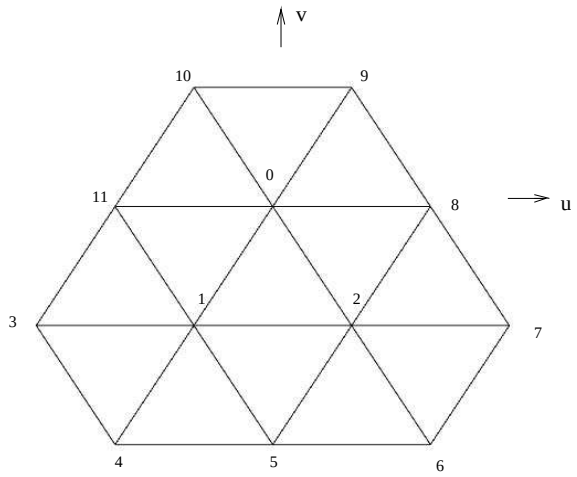

Figure 2.7: The grid in R^2 contains all vertices that have influence on the surface patch corresponding to the center triangle. Each vertex is associated with a specific nodal function.

where p_i is the control point of the patch and ξ_i is the nodal function corresponding to p_i, $i = 0, \ldots, \mu$ and μ is the number of control points of the patch.

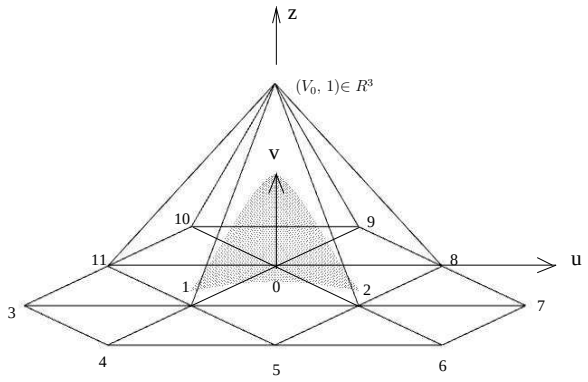

Figure 2.8: We associate one with v_0 and zero with all other vertices. The shaded area over the center triangle 0-1-2 (see Figure 2.7) corresponds to the approximation of the nodal function ξ_0 associated with v_0. That is to say, for a point over the center triangle defined in Figure 2.7, the components u and v of the point correspond to one (u, v) coordinate and the component z is the nodal function for this (u, v) coordinate.

With the pre-computed nodal functions, the evaluation of the patch is simple and straightforward:

$$s(u,v) = \sum_{i=0}^{\mu} \xi_i(u,v) p_i$$

where p_i is the control point of the patch and ξ_i is the nodal function corresponding to p_i, $i = 0, \ldots, \mu$ and μ is the number of control points of the patch.

Parametrization

The parametrization of the Loop patch is the fundamental step of the Wu-Peters method. The so-called exact parametrization of the Loop patch by Wu-Peters is defined by the following construction (cf. Figure 2.9):

1. Set v_0 to be the origin of the (u, v) plane.
2. The direct neighbors v_i of v_0 form a regular unit n-gon.
3. Extend the edges v_0v_1 and v_0v_2 by k_n to get v_4 and v_6.
4. v_5 is the average of v_4 and v_6.
5. v_3, v_7 are the reflection of v_5, across v_0v_4 and v_0v_6.

k_n is defined by the following formula:

$$k_n := \begin{cases} -4(c^2-2)/(1+2c^2) - 1 & \text{if } n \geq 6 \\ -6(2c^2-7)/(15+2c^2) - 1 & \text{if } n < 6 \end{cases}$$

where $c := \cos\frac{\pi}{n}$.

The domain Ω_n of the Loop patch is the limit of the subdivision applied to the initial mesh of the abscissae v_i [2, Sec. 6.5]. We choose the abscissae mesh to be symmetric with respect to the extraordinary node. The Ω_n falls into the sector formed by the initial abscissa triangle $\triangle_n$ with vertices v_0, v_1, v_3 (see Figure 2.9) [24].

As mentioned above, the purpose of the parametrization is to ensure that the domain of the patch is strictly within the center triangle. This can be done, in the case $n \geq 6$, if v_i is mapped into v_i (the limit positions are equal to their original positions), $i = 0, 1, 2$; in the case $3 \leq n \leq 5$, let v_m be the middle point between v_1 and v_2; in this case the v_i are chosen so that the limit position of v_m is $\frac{1}{2}(v_1 + v_2)$. The proof that the vertices, given in the itemized list above, give the desired limit positions, is given below.

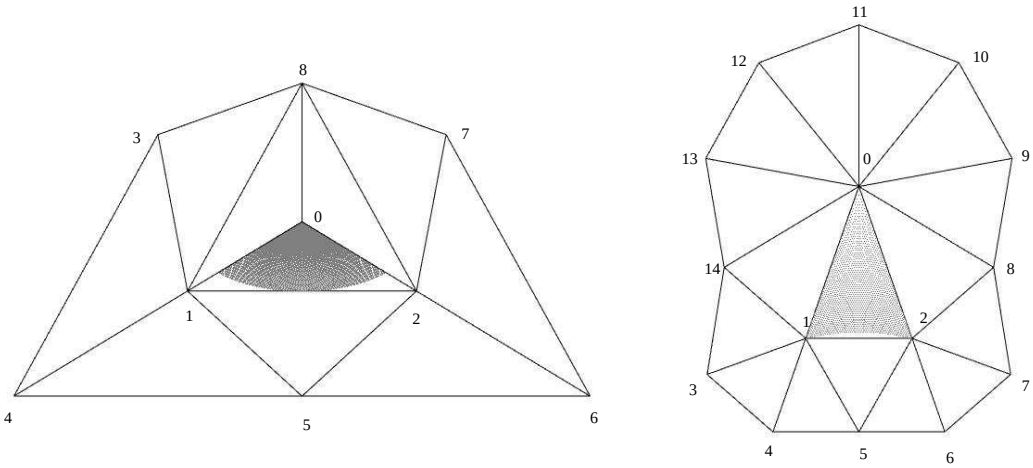

(a) n=3 (b) n=9

Figure 2.9: Shaded areas are the domains of the patches.

Wu-Peters also presented another parametrization: uniform parametrization. With the same construction as above, but with $k_n = 1$ for all n, we obtain the uniform parametrization. The bottom boundary of the domain will either, for $n < 6$, pull back from the boundary of the center triangle or, for $n > 6$, push out of the center triangle. Therefore, for $n < 6$, we have a large overestimate due to the larger gap between the center triangle and the domain compared to the exact parametrization, while for $n > 6$, we cannot have a guaranteed bounding volume to envelope the limit surface as the domain pushes out of the center triangle (see Figure 2.10).

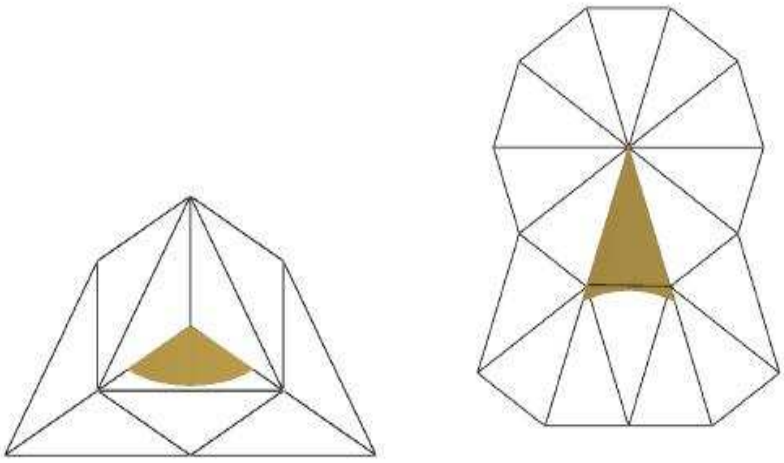

Figure 2.10: The domains of uniform parametrization with $n = 3$ (left) and $n = 9$ (right).

One technique that will be used to establish appropriate values of the constants in the exact parametrization is to compute the limit positions directly from the control point p_i^m on some levels m without going through the iterative refinement. The standard technique in the analysis of subdivision schemes is:

1. Construct a local subdivision matrix.

2. Transform the local subdivision matrix into basis of eigenvectors.

Because our Loop patch has at most one extraordinary vertex and only v_0 is possibly an extraordinary vertex, we just need the local subdivision matrix for regular vertices.

The local subdivision matrix for a regular vertex is [18]:

$$\tilde{S} = \frac{1}{16}\begin{pmatrix} 10 & 1 & 1 & 1 & 1 & 1 & 1 \\ 6 & 6 & 2 & 0 & 0 & 0 & 2 \\ 6 & 2 & 6 & 2 & 0 & 0 & 0 \\ 6 & 0 & 2 & 6 & 2 & 0 & 0 \\ 6 & 0 & 0 & 2 & 6 & 2 & 0 \\ 6 & 0 & 0 & 0 & 2 & 6 & 2 \\ 6 & 2 & 0 & 0 & 0 & 2 & 6 \end{pmatrix},$$

which can be decomposed into $\tilde{S} = V^{-1}DV$ by singular value decomposition, where

$$V^{-1} = \begin{pmatrix} 1 & 0 & 0 & 0 & 0 & 1 & 0 \\ 1 & 1 & -1 & 0 & 1 & 0 & -1 \\ 1 & 0 & -1 & -1 & -1 & -3 & -1 \\ 1 & -1 & 0 & 1 & 0 & 0 & -1 \\ 1 & -1 & 1 & 0 & 1 & 0 & 1 \\ 1 & 0 & 1 & -1 & -1 & -3 & -1 \\ 1 & 1 & 0 & 1 & 0 & 0 & 1 \end{pmatrix},$$

$$D = \frac{1}{16} \begin{pmatrix} 16 & 0 & 0 & 0 & 0 & 0 & 0 \\ 0 & 8 & 0 & 0 & 0 & 0 & 0 \\ 0 & 0 & 8 & 0 & 0 & 0 & 0 \\ 0 & 0 & 0 & 4 & 0 & 0 & 0 \\ 0 & 0 & 0 & 0 & 4 & 0 & 0 \\ 0 & 0 & 0 & 0 & 0 & 4 & 0 \\ 0 & 0 & 0 & 0 & 0 & 0 & 2 \end{pmatrix},$$

$$V = \frac{1}{12} \begin{pmatrix} 6 & 1 & 1 & 1 & 1 & 1 & 1 \\ 0 & 2 & -2 & -4 & -2 & 2 & 4 \\ 0 & -2 & -4 & -2 & 2 & 4 & 2 \\ -6 & -1 & -1 & 5 & -1 & -1 & 5 \\ -6 & 5 & -1 & -1 & 5 & -1 & -1 \\ 6 & -1 & -1 & -1 & -1 & -1 & -1 \\ 0 & -2 & 2 & -2 & 2 & -2 & 2 \end{pmatrix}.$$

The first row of the matrix V is the left eigenvector which will be used as the mask to compute the vertex's limit position of Loop subdivision scheme without iterative refinement step.

We now have the regular vertex limit position mask [17]:

$$\left(\frac{6}{12}, \frac{1}{12}, \frac{1}{12}, \frac{1}{12}, \frac{1}{12}, \frac{1}{12}, \frac{1}{12}\right).$$

Having the limit position mask for regular vertex of the Loop subdivision scheme, we can compute the parameters of exact parametrization for the Loop scheme [2, Sec. 6.8].

First, we consider the case $n \geq 6$. To envelop the limit surface of one Loop patch, we need to consider v_0, v_1, and v_2 (see Figure 2.9). The limit position of v_0 is always equal to its original position by the central symmetry of its one-ring neighbors. For v_1 and v_2, we should adjust their one-ring neighbors' positions to assure their limit positions are equal to their original positions; since v_1 and v_2 are regular vertices, we can use the above limit position mask.

First, we consider v_2; the one-ring neighbors of v_2 are v_0, v_1, v_5, v_6, v_7, and v_8.

To fix v_2, we have the following formula by the limit position mask:

$$v_2 = \frac{6}{12}v_2 + \frac{1}{12}(v_0 + v_1 + v_5 + v_6 + v_7 + v_8). \tag{2.1}$$

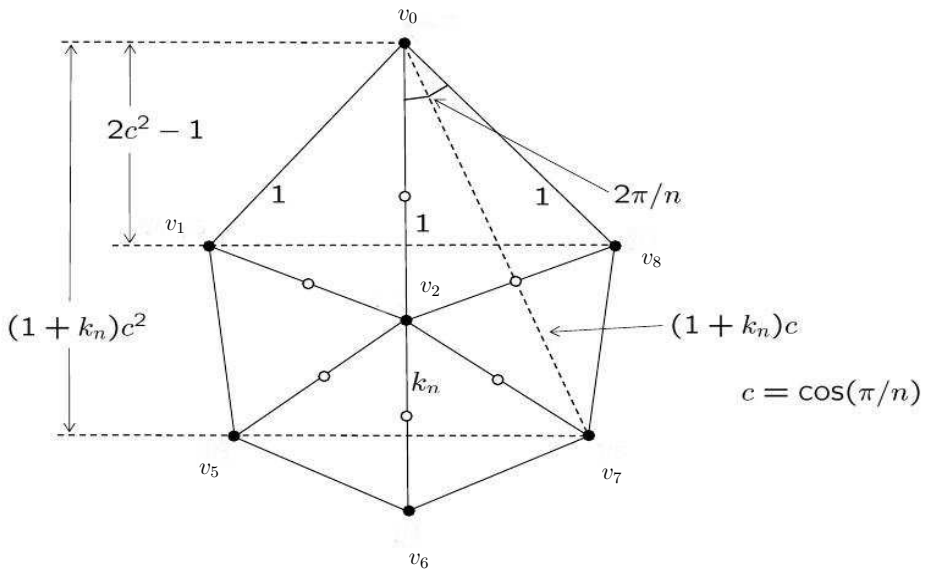

Figure 2.11: Rotated planar grid.

For easier computation, we rotate the planar grid in Figure 2.9 by α_n (see Figure 2.11, which is valid for all $n > 6$.). It is clear by symmetry that the horizontal component of the average of the points v_0, v_1, v_5, v_6, v_7, and v_8 is equal to the horizontal component of v_2. So we just need to consider the vertical components.

The vertical component of

$$\begin{array}{lll} v_0 & \text{is} & 0, \\ v_1 & \text{is} & 1 - 2c^2, \\ v_{n+5} & \text{is} & -\cos(2\pi/n) = 1 - 2\cos^2(\pi/n) = 1 - 2c^2, \\ v_2 & \text{is} & -1, \\ v_7 & \text{is} & -(1 + k_n)c^2 \text{ (since } v_0v_7 \text{ has length } (1 + k_n)\cos(\pi/n)), \\ v_5 & \text{is} & -(1 + k_n)c^2, \\ v_6 & \text{is} & -(1 + k_n). \end{array}$$

With the vertical components of $v_0, v_1, v_2, v_5, v_6, v_7$, and v_8, we transform Equation (2.1) into

$$-1 = -\frac{1}{2} + \frac{1}{12}(1 - 2c^2 + 1 - 2c^2 - 2(1 + k_n)c^2 - 1 - k_n), \tag{2.2}$$

$$\implies 6c^2 + 2c^2k_n + k_n = 7, \tag{2.3}$$

$$\Longrightarrow\ k_n = \frac{-4(c^2-2)}{2c^2+1} - 1 \tag{2.4}$$

where $c = \cos(\frac{\pi}{n})$ and $n \geq 6$. Consequently, this choice of k_n [24] ensures that the limit position of v_2 is equal to its origin position.

Now consider the case $3 \leq n \leq 5$. In this case, it is not necessary to rotate the coordinate system in Figure 2.9. It is clear by symmetry that the horizontal component of the limit position v_m is equal to the horizontal component of $\frac{1}{2}(v_1 + v_2)$ where v_m is the middle point between v_1 and v_2. The vertex v_m is influenced at the next subdivision step by the same vertices of the patches with valences $3 \leq n \leq 5$ (see Figure 2.12 and Figure 2.13 where the $v^{'}$ denote the values at the next subdivision step). Let $\alpha_n = \pi/n$, $c = \cos(\pi/n) = \cos\alpha_n$. The vertical components of

v_0	is	0,
v_1, v_2	are	$-c$ ($c > 0$ since $\pi/n < \pi/2$),
v_4, v_5, v_6	are	$\sin(3\pi/2 - \alpha_n)(1 + k_n) = -c(1 + k_n)$,
v_3, v_7	are	$-\sin(3\pi/2 - 2\pi/n)[\sin(3\pi/2 - \alpha_n)(1 + k_n)] = -2(c^2 - 1)c(1 + k_n)$,
v_8 ($n = 3$)	is	$\sin(3\pi/2 + 2\pi/n + \pi/n) = -4(4c^3 - 3c)$,
v_8, v_9 ($n = 4$)	is	$\sin(3\pi/2 + 2\pi/n + \pi/n) = -4(4c^3 - 3c)$,
v_8, v_{10} ($n = 5$)	is	$\sin(3\pi/2 + 2\pi/n + \pi/n) = -4(4c^3 - 3c)$,
v_m	is	$3/8(-2c) + 1/8(-c(1 + k_n)) = -c/8(7 + k_n)$.

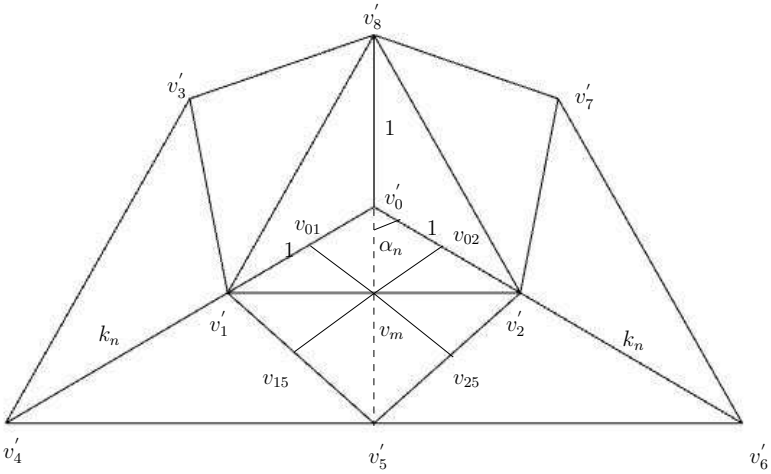

Figure 2.12: The patches with valence $n = 3$.

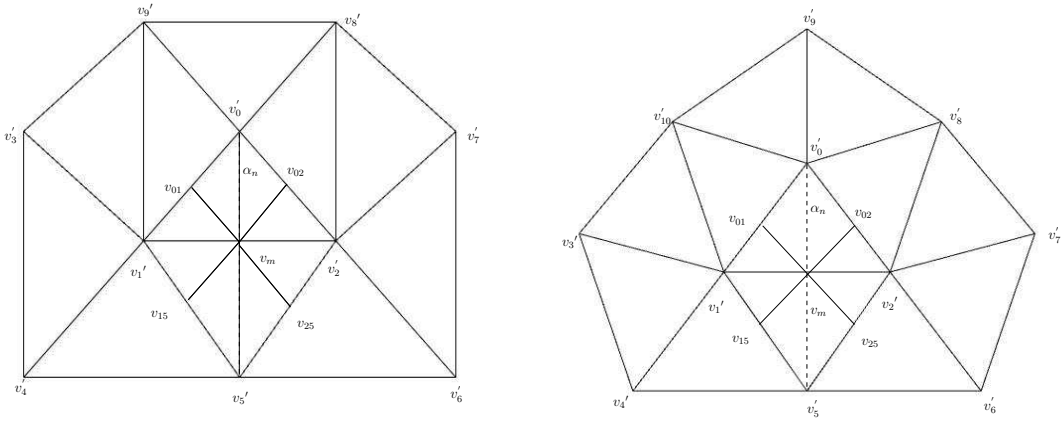

Figure 2.13: The patch with valences $n = 4$ and $n = 5$.

Since v_m is a regular vertex, the limit position of v_m is computed as $\frac{1}{2}v_m + \frac{1}{2}v_{avg}$, where v_{avg} is the average of the six neighbors of v_m after the first subdivision step. Its neighbors are

$$\begin{aligned}
v_{01} &= 3/8(v_0 + v_1) + 1/8(v_2 + v_{n+5}),\\
v_{15} &= 3/8(v_1 + v_5) + 1/8(v_2 + v_4),\\
v_{25} &= 3/8(v_2 + v_5) + 1/8(v_1 + v_6),\\
v_{02} &= 3/8(v_0 + v_2) + 1/8(v_1 + v_8),\\
v_1^{'} &= (5/8)v_1 + (1/6)(3/8)(v_0 + v_{n+5} + v_3 + v_4 + v_5 + v_2),\\
v_2^{'} &= (5/8)v_2 + (1/6)(3/8)(v_0 + v_1 + v_5 + v_6 + v_7 + v_8).
\end{aligned}$$

A straightforward calculation now shows that the vertical component of $v_m = \frac{1}{2}v_m + \frac{1}{2}v_{avg} = -c$ and with the six neighbors of v_m, we have the equation:

$$v_m = \frac{1}{2}v_m + \frac{1}{2}v_{avg}, \tag{2.5}$$

$$\implies v_m = \frac{1}{2}v_m + \frac{1}{12}(v_{01} + v_{15} + v_{25} + v_{02} + v_1^{'} + v_2^{'}), \tag{2.6}$$

$$\implies 189v_1 + 3v_3 + 48v_5 + 9v_8 = 288v_m, \tag{2.7}$$

$$\implies k_n(2c^2 + 15) = 27 - 14c^2, \tag{2.8}$$

$$\implies k_n = \frac{-6(2c^2 - 7)}{15 + 2c^2} - 1, \tag{2.9}$$

where $c = \cos(\frac{\pi}{n})$ and $3 \leq n \leq 5$. Consequently, this choice [24] ensures that the limit position of v_m is equal to its origin position.

Chapter 3

Catmull-Clark and 4-8 Subdivision

Since it was introduced by Edwin Catmull and Jim Clark in 1978, the Catmull-Clark subdivision method [7] has become a graphics-industry standard. As one of the first surface subdivision methods, it is also widely used in the study of properties of subdivision surfaces.

In 2000, Luiz Velho and Denis Zorin introduced the 4-8 subdivision method [23]. This method has the advantage that it uses bisection refinement as elementary refinement operation, rather than the commonly used face or vertex splits. Because 4-8 meshes are refinable *triangulated quadrangulations*, they provide a powerful hierarchical structure for multi-resolution applications.

While the Catmull-Clark subdivision method is widely used in the graphics industry, the 4-8 method is a newer method which has several advantages. But there is a common challenge for the two methods: how to construct simple and efficient bounding volumes for the patches of the subdivision surfaces. In the next chapter, we will introduce a method which extends the method of Wu-Peters [24] which was derived for the Loop method, to the parametric surfaces of Catmull-Clark and 4-8 subdivision. Before doing the extension of the Wu-Peters method, we should have a good understanding of Catmull-Clark and 4-8 subdivision.

3.1 Catmull-Clark Subdivision

The Catmull-Clark method generalizes the uniform *bicubic* B-spline, which is the tensor product of two cubic B-splines. The Catmull-Clark subdivision method belongs to the class of primal methods, which use rules that work directly with the mesh defined in terms of its vertices, edges and faces. One important type of *splitting* used in this context is quadrilateral splitting, the *pQ4* splitting schema [16] described in Section 3.1.1 below. In particular, this is the splitting schema used by the Catmull-Clark method. A vertex with valence $n \neq 4$ is called an *extraordinary vertex*, and a face with a number of edges $e \neq 4$ is called an *extraordinary face*. No extraordinary faces will remain in the mesh after the first subdivision step, and no extraordinary vertices will be introduced after the first subdivision step.

The subdivision rules for computing face points, edge points and vertex points are given as follows [7]:

1. A new face point is the average of all old points defining the face.

2. Each edge point is equal to the average of the midpoint of the old edge with the average of the two new face points of the two incident faces.

3. A vertex point is updated by the average $\frac{1}{n}[(n-3)V + 2R + Q]$, where V is the old vertex of valence n, R is the average of the midpoints of all old edges sharing the vertex, and R is the average of the new face points of all faces adjacent to the vertex.

As one of the first surface subdivision methods introduced, there are many different descriptions of the method in the literature [2, Sec. 8.1].

Jos Stam [22] extended the Catmull-Clark method to generalize uniform tensor product B-spline surfaces of any bi-degree to meshes of arbitrary topology. This method uses only one-ring neighborhoods.

Subdivision methods consume a lot of memory, so a method permitting in-place computation will be a good choice. We will see in the following sections that the realization of in-place computation for the Catmull-Clark subdivision method is very easy.

In the following two sections, we give a fairly detailed introduction to two versions of the Catmull-Clark subdivision method based on the book [2]:

1. Linear-Subdivision plus Smoothing formulation (LSS formulation)

2. In-place formulation.

More detailed information about the Catmull-Clark subdivision method and other subdivision methods is available in this book.

3.1.1 Catmull-Clark (LSS formulation)

The presentation of the LSS (Linear-Subdivision plus Smoothing) formulation of the Catmull-Clark algorithm is based on ideas of Stam [22] and Zorin and Schröder [27], while the formulation in Section 3.1.2 is very close to the original description of [7].

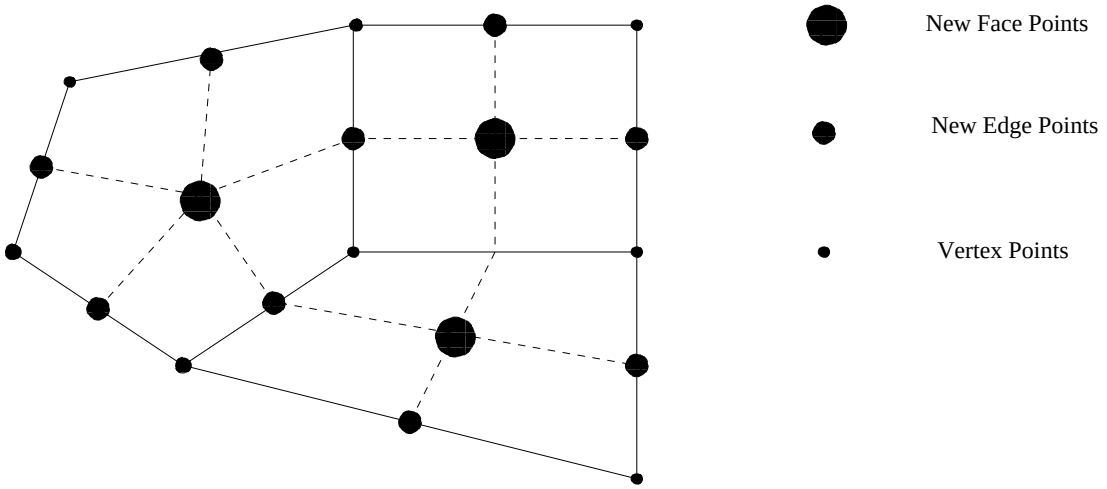

Figure 3.1: Result of subdivision using $pQ4$ scheme.

The Catmull-Clark method begins by refining the mesh according to the $pQ4$ schema (see Figure 3.1):

1. Each edge is subdivided to create a new vertex (edge vertex) in the middle of the edge.

2. A new vertex (face vertex) is added in the middle of each face.

3. This new face vertex is joined to each of the new edge vertices.

The refinement of the mesh is followed by assignment of geometric data to the newly added vertices, and modification of the geometric data associated with existing vertices. Here we have distinguished between the logical vertices in the mesh and the geometric

data associated with these vertices. It is standard in the subdivision literature, however, to refer to them together as a point. Thus, for example, in Figure 3.1, "Vertex Point" refers to an existing logical vertex for which the associated geometric data must be modified.

The LSS formulation [22] of the Catmull-Clark method is a very natural description of the method, and it is very close to the fundamental Lane-Riesenfeld algorithm on which the Catmull-Clark method is based. This formulation consists of two sub-steps:

1. The polyhedral mesh is *linearly subdivided*, which means that the *new face point* is assigned the value equal to the centroid of the face and the *new edge point* is assigned the value equal to the average of the two control points at its two neighboring vertices.

2. Each point (including *new face points* and *new edge points*) in the subdivided mesh is smoothed using the mask shown in Figure 3.2.

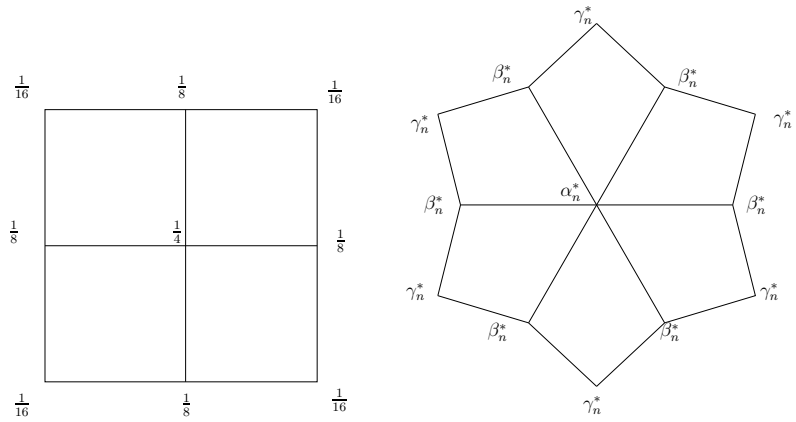

Figure 3.2: Catmull-Clark smoothing mask with $n = 4$ and $n = 6$.

The weights of the Catmull-Clark smoothing masks are defined by

$$\alpha_n^* = \frac{n-3}{n}, \quad \beta_n^* = \frac{2}{n^2}, \quad \gamma_n^* = \frac{1}{n^2}.$$

3.1.2 Catmull-Clark (In-place formulation)

For most common quadrilateral subdivision schemes, a single uniform refinement step increases the number of faces or vertices by a factor 4. Consequently, the implementations of subdivision methods will need much memory. An *in-place* formulation means

that during the refinement of a given mesh, we do not need to create temporary vertices to store data. In this case, we can save a lot of memory and improve the performance.

An in-place version of the Catmull-Clark computation is very easy to obtain. We just perform the calculations in a different order compared to the LSS formulation. Assume that the current values of V, E_i and F_i are stored, that memory has been allocated for each new face point (denoted $F_i^{'}$) and each new edge point (denoted $E_i^{'}$). Then the computation can be done in the following order:

1. Compute $F_i^{'}$: $F_i^{'}$ is the centroid of the face's old vertex points:

   $F_i^{'} \leftarrow \frac{1}{4}[V + E_i + F_i + E_{i+1}]$ if the face is quadrilateral.

2. Compute $E_i^{'}$ (preliminary value): $E_i^{'} \leftarrow \frac{1}{2}[V + E_i]$.

3. Smooth the vertex point $V^{'}$: $V^{'} \leftarrow \alpha_n^* V + n\beta_n^* R + n\gamma_n^* Q$.

4. Compute $E_i^{'}$ (final value): $E_i^{'} \leftarrow \frac{1}{2}[E_i^{'} + \frac{1}{2}(F_{i-1}^{'} + F_i^{'})]$.

In step 3, R is the average of the midpoints of all edges (values are available from step-2) incident to the vertex, Q is the average of the new face points (values are available from step-1) of all faces incident to the vertex, where

$$\alpha_n^* = \frac{n-3}{n}, \quad \beta_n^* = \frac{2}{n^2}, \quad \gamma_n^* = \frac{1}{n^2}.$$

The only difference between the in-place version and the original Catmull-Clark formulation [7] is the order of computation.

We can easily prove that the in-place formulation of Catmull-Clark is exactly equivalent to the LSS formulation.

1. Computation of *Face Points* in the *in-place* formulation:

   $$F_i^{'} \leftarrow \frac{1}{4}[V + E_i + F_i + E_{i+1}] \quad i = 0, \ldots, n-1.$$

   The first step of computing *Edge Points* of *in-place* formulation is

   $$E_i^{'} \leftarrow \frac{1}{2}[V + E_i] \quad i = 0, \ldots, n-1.$$

   These two computations are exactly the same thing as the first step of the LSS formation.

2. Smooth the vertices V in the LSS formulation:

$$V' \leftarrow \alpha_n^* V + \beta_n^* \left[\sum_{j=0}^{n-1} \frac{1}{2}(V + E_j)\right] + \gamma_n^* \left[\sum_{j=0}^{n-1} \frac{1}{4}(V + E_j + F_j + E_{j+1})\right],$$

which can be written as

$$V' \leftarrow \alpha_n^* V + n\beta_n^* R + n\gamma_n^* Q.$$

This is the same thing as step 3 of the *in-place* formulation.

3. Smooth the *Edge Points* E_i' in the LSS formulation:

$$\begin{aligned} E_i' &= \frac{1}{4}\left[\frac{1}{2}(V + E_i)\right] \\ &\quad + \frac{1}{8}\left[V + \frac{1}{4}(V + E_{i-1} + F_{i-1} + E_i) + E_i + \frac{1}{4}(V + E_i + F_i + E_{i+1})\right] \\ &\quad + \frac{1}{16}\left[\frac{1}{2}(V + E_{i-1}) + \frac{1}{2}(E_i + F_{i-1} + \frac{1}{2}(E_i + F_i) + \frac{1}{2}(V + E_{i+1})\right] \\ &= \frac{3}{8}(V + E_i) + \frac{1}{16}(E_{i-1} + F_{i-1} + F_i + E_{i+1}). \end{aligned}$$

This is the same thing as step 4 of the *in-place* formulation.

4. Smooth the *Face points* in the LSS formulation:

$$\begin{aligned} F_i' &= \frac{1}{4}\left[\frac{1}{4}(V + E_i + F_i + E_{i+1})\right] \\ &\quad + \frac{1}{8}\left[\frac{1}{2}(V + E_i) + \frac{1}{2}(E_i + F_i) + \frac{1}{2}(F_i + E_{i+1}) + \frac{1}{2}(E_{i+1} + V)\right] \\ &\quad + \frac{1}{16}\left[V + E_i + F_i + E_{i+1}\right] \\ &= \frac{1}{4}\left[V + E_i + F_i + E_{i+1}\right]. \end{aligned}$$

This is exactly the same thing as the first step of the *in-place* formulation.

3.1.3 Ball-Storry Formulation

We also present the Ball-Storry formulation of the Catmull-Clark method [4], because we use this formulation in our project. We can construct the local subdivision matrix explicitly using the Ball-Storry formulation.

In the project, we are interested in computing the limit points directly from the control points p_i^m on some level m without going through the iterative refinement. Since

the local subdivision matrix controls the behavior of the surface in a neighborhood of the vertices of the mesh, it comes as no surprise that many properties of subdivision surfaces can be inferred from the properties of the local subdivision matrix [23]. The standard technique of the analysis of subdivision methods is:

1. Construct a *local subdivision matrix*.

2. Transform it into its basis of eigenvectors.

Assume $\tilde{S}$ is a local subdivision matrix, the direct computation of the limit positions of the control points p_i^m on some level m can be done using the decomposition of $\tilde{S} = V^{-1}DV$ into a diagonal matrix D and a basis of left eigenvectors [2, Sec. 5.4]. The convergence of the iterative scheme implies the affine invariance of the subdivision scheme [2], which means that the dominant eigenvalue of $\tilde{S}$ is $\lambda_1 = 1$ and that corresponding eigenvector is $[1, ..., 1]^T$. The first column of V^{-1} is associated with this eigenvalue.

Now we present the Ball-Storry formulation and verify that it produces the same result as the two formulations we have presented. We can write the new vertex point of Ball-Storry formulation in an inner-product-like notation [2]:

$$\left[\frac{4n-7}{4n} \quad \frac{3}{2n} \quad \frac{1}{4n}\right] \cdot \left[V \; \frac{1}{n}\sum_{j=0}^{n-1} \quad \frac{1}{n}\sum_{j=0}^{n-1} F_j\right]$$

Now we prove that the Ball-Storry formulation produces the same result as the two previous formulations.

1. Compute $F^{'}$

$$F^{'} \leftarrow \frac{1}{4}(V + E_j + F_j + E_{j+1}),$$

   which is the same computation as two previous formulations.

2. Compute $E^{'}$

$$E^{'} \leftarrow \frac{3}{8}(V + E_j) + \frac{1}{16}(E_{j_1} + F_{j-1} + F_j + E_{j+1}).$$

   We can verify in a straightforward way that this is the same computation as in the previous formulations.

3. Smoothing the vertex points V'

$$V' \leftarrow \alpha_n V + \beta_n \left(\frac{1}{n} \sum_{j=0}^{n-1} E_j \right) + \gamma_n \left(\frac{1}{n} \sum_{j=0}^{n-1} F_j \right)$$

where

$$\alpha_n = \frac{4n-7}{4n}, \quad \beta_n = \frac{3}{2n}, \quad \gamma_n = \frac{1}{4n}.$$

We can also verify that this is the same computation as two previous formulations, as follows. In the original form [7] of the method, the smoothing of a vertex point was defined as

$$\begin{aligned} V' &= \left(\frac{n-3}{n}\right) S + \left(\frac{2}{n}\right) R + \left(\frac{1}{n}\right) Q \\ &= \left(\frac{n-3}{n}\right) V + \frac{1}{n^2} \sum_{j=0}^{n-1} (V + E_j) + \frac{1}{4n^2} \sum_{j=0}^{n-1} (V + E_j + F_j + E_{j+1}) \\ &= \left(\frac{4n-7}{4n}\right) V + \frac{3}{4n} \sum_{j=0}^{n-1} E_j + \frac{1}{4n} \sum_{j=0}^{n-1} F_j \end{aligned}$$

where

$$\begin{aligned} S &= V \\ R &= \tfrac{1}{n} \textstyle\sum_{j=0}^{n-1} \tfrac{1}{2} (V + E_j) \\ Q &= \tfrac{1}{n} \textstyle\sum_{j=0}^{n-1} F'_j. \end{aligned}$$

Now we can obtain the local subdivision matrix [26, Sec. 3.3] of the Catmull-Clark scheme for the regular case (valence of the vertex is 4).

$$\tilde{S} = \frac{1}{64} \begin{pmatrix} 36 & 6 & 6 & 6 & 6 & 1 & 1 & 1 & 1 \\ 24 & 24 & 4 & 0 & 4 & 4 & 0 & 0 & 4 \\ 24 & 4 & 24 & 4 & 0 & 4 & 4 & 0 & 0 \\ 24 & 0 & 4 & 24 & 4 & 0 & 4 & 4 & 0 \\ 24 & 4 & 0 & 4 & 24 & 0 & 0 & 4 & 4 \\ 16 & 16 & 16 & 0 & 0 & 16 & 0 & 0 & 0 \\ 16 & 0 & 16 & 16 & 0 & 0 & 16 & 0 & 0 \\ 16 & 0 & 0 & 16 & 16 & 0 & 0 & 16 & 0 \\ 16 & 16 & 0 & 0 & 16 & 0 & 0 & 0 & 16 \end{pmatrix},$$

which can be decomposed into $\tilde{S} = V^{-1} D V$, where

$$V^{-1} = \begin{pmatrix} 1 & 0 & 0 & -2 & -2 & -2 & 0 & 0 & 1 \\ 1 & 3 & -3 & 1 & 1 & -8 & -3 & 3 & -2 \\ 1 & -3 & -3 & 1 & 1 & 10 & 3 & 3 & -2 \\ 1 & -3 & 3 & 1 & 1 & -8 & 3 & -3 & -2 \\ 1 & 3 & 3 & 1 & 1 & 10 & -3 & -3 & -2 \\ 1 & 0 & -6 & -5 & 13 & 4 & 0 & -12 & 4 \\ 1 & -6 & 0 & 13 & -5 & 4 & -12 & 0 & 4 \\ 1 & 0 & 6 & -5 & 13 & 4 & 0 & 12 & 4 \\ 1 & 6 & 0 & 13 & -5 & -4 & 12 & 0 & 4 \end{pmatrix},$$

$$D = \frac{1}{16}\begin{pmatrix} 16 & 0 & 0 & 0 & 0 & 0 & 0 & 0 & 0 \\ 0 & 8 & 0 & 0 & 0 & 0 & 0 & 0 & 0 \\ 0 & 0 & 8 & 0 & 0 & 0 & 0 & 0 & 0 \\ 0 & 0 & 0 & 4 & 0 & 0 & 0 & 0 & 0 \\ 0 & 0 & 0 & 0 & 4 & 0 & 0 & 0 & 0 \\ 0 & 0 & 0 & 0 & 0 & 4 & 0 & 0 & 0 \\ 0 & 0 & 0 & 0 & 0 & 0 & 2 & 0 & 0 \\ 0 & 0 & 0 & 0 & 0 & 0 & 0 & 2 & 0 \\ 0 & 0 & 0 & 0 & 0 & 0 & 0 & 0 & 1 \end{pmatrix},$$

$$V = \frac{1}{36}\begin{pmatrix} 16 & 4 & 4 & 4 & 4 & 1 & 1 & 1 & 1 \\ 0 & 2 & -2 & -2 & 2 & 0 & -1 & 0 & 1 \\ 0 & -2 & -2 & 2 & 2 & -1 & 0 & 1 & 0 \\ -4 & 1 & 0 & 1 & 0 & 0 & 1 & 0 & 1 \\ -4 & 1 & 0 & 1 & 0 & 1 & 0 & 1 & 0 \\ 0 & -1 & 1 & -1 & 1 & 0 & 0 & 0 & 0 \\ 0 & -1 & 1 & 1 & -1 & 0 & -1 & 0 & 1 \\ 0 & 1 & 1 & -1 & -1 & -1 & 0 & 1 & 0 \\ 4 & -2 & -2 & -2 & -2 & 1 & 1 & 1 & 1 \end{pmatrix}.$$

The first row of the matrix V is the left eigenvector, which will be used as the mask to compute the vertex's limit position of the Catmull-Clark subdivision scheme, in the chapter on the parametrization of subdivision surfaces.

3.2 4-8 Subdivision

The 4-8 subdivision scheme was proposed by Luiz Velho and Denis Zorin [23] in 2001. This method generalizes the four directional box spline of class C^4 [2, Sec. 3] to surfaces of arbitrary topological type. Recall that an important part of the definition of a subdivision scheme is the refinement rule, as in the Catmull-Clark subdivision scheme which is based on the *pQ4* [16] scheme, the Loop subdivision scheme which is based on the *pT4* [16] scheme and the Doo-Sabin schema which is based on the *dQ4* [16] scheme. As mentioned above, one of the advantages of the 4-8 subdivision scheme is that it uses bisection refinement as an elementary refinement operation, rather than the more commonly used face or vertex splits of the Catmull-Clark, Doo-Sabin or Loop subdivision schemes.

The 4-8 subdivision scheme has several advantages [23]:

1. *The basic refinement operation is bisection.* The result of applying a single bisection to a conforming mesh [19] is a conforming mesh: no cracks can appear. This simplifies adaptive refinement.

2. *Gradual refinement.* The splitting scheme increases the number of faces by only a factor of 2 at each refinement step. In contrast, for the Catmull-Clark case, the increase is a factor of 4.

3. *Small support and high smoothness.* The support for a vertex mask is smaller than that of the Catmull-Clark scheme (smaller support implies less computation) and the support for a face mask is the same. The resulting surface is C^4-continuous on the regular mesh, which is higher than the Catmull-Clark subdivision, which is only C^2-continuous.

4. *High symmetry.* The basis function in the regular case is invariant with respect to rotations by $\pi/8$; thus it has a larger symmetry group compared to basis functions of tensor-product and three-directional box splines.

3.2.1 4-8 Meshes and Refinement

In this section we introduce the basic concepts of regular 4-8 meshes and bisection refinement.

Typical mesh refinement methods are closely related to regular tilings. A tiling is said to be regular if every vertex has a fixed number of incident vertices. There are only three types of regular plane tilings [12]; the tile has to be either a square, an equilateral triangle, or a regular hexagon. Most known refinement schemes are based on square or triangular tilings.

The 4-8 subdivision scheme is based on a different plane tiling namely one of the *monohedral tilings* with regular vertices, also known as *Laves tilings*, named after the crystallographer Fritz Laves [12].

In a *monohedral tiling*, every tile is congruent to one fixed tile, called the *prototile*. The prototile of the $[4.8^2]$ Laves tiling is an isosceles right triangle. We call it the 4-8 tiling as it has alternating vertices of valence 4 and 8 (see Figure 3.3). Here are some definitions used in 4-8 meshes [23] (we assume that the 4-8 mesh is made up of quadrilaterals, this can be done by applying one Catmull-Clark subdivision step to the 4-8 mesh):

1. *Basic block.* The basic structure of 4-8 tiling is a pair of triangles forming a block divided along one of its diagonals. We call this structure a *basic block*. A 4-8 mesh

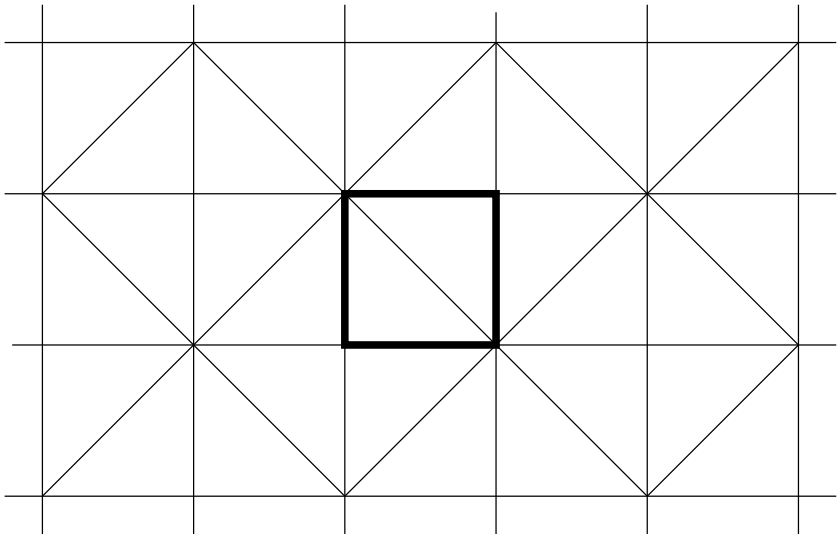

Figure 3.3: Laves $[4.8^2]$ tilings with one of the basic blocks outlined.

is made up of basic blocks.

2. *Interior edge.* We call the common edge of the two triangles of the block an *interior edge.*

3. *Exterior edge.* We call all other edges of 4-8 meshes *exterior edges.*

4. *Tri-quad mesh.* The 4-8 tiling forms a *triangulated quadrangulation.* We also call a 4-8 mesh a *tri-quad mesh.*

A regular 4-8 mesh has the same block structure as the 4-8 tiling. The basic structure of a 4-8 mesh is formed by two triangles. Each triangle has a single interior edge and two exterior edges. We use *bisection* as a primitive refinement operation: we bisect only the interior edge of each block.

We have said that the important advantage of the 4-8 subdivision scheme is that it uses bisection refinement as an elementary refinement operation. We introduce the bisection refinement operation for the regular case (see Figure 3.4):

1. Add a split vertex on interior edges of blocks.

2. Subdivide each face into two sub-faces and link the split vertex on the interior edge to the opposite vertex of the face.

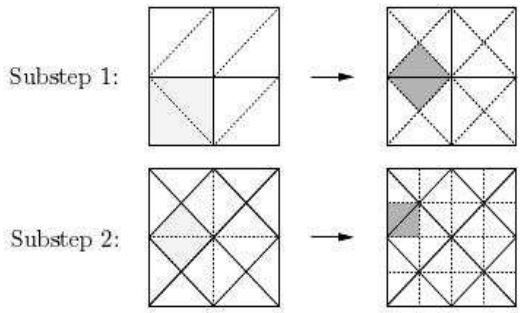

Figure 3.4: Two bisections in the regular case [2, Sec. 3.7].

Bisection refinement is used in a 4-8 mesh. Each 4-8 subdivision step is made up of two consecutive bisection sub-steps. We need to produce a 4-8 mesh from a given mesh. Bisection refinement can be applied to an arbitrary mesh partitioned into blocks of two triangles sharing an edge. In our project, the initial mesh is a quadrilateral mesh, so we just split each quad into two triangles to produce tri-quad meshes.

3.2.2 Definition of 4-8 Subdivision

In this section we define the 4-8 subdivision scheme based on bisection refinement for computing positions of the new face vertices of the basic blocks and updating the positions of the existing vertices. We can classify these definitions into two classes: face rule and vertex rule. The same rules are used in each bisection sub-step.

1. *Face rule*: Each new face vertex inserted into the basic block is computed as the barycenter of the block.

2. *Vertex rule*: The new position of an existing vertex v is computed as the average of the old position and barycenter of the vertices sharing an exterior edge with v.

The 4-8 regular mesh is a tri-quad mesh which has only vertices of valences 4 and 8 and the one-neighborhood of every internal vertex of valence 4 has only neighbors of valence 8, and the one-neighborhood of every internal vertex of valence 8 consists of one-ring of vertices with alternating valences 4 and 8.

We have an important observation about the vertices:

1. A vertex added by a refinement step has valence 4.

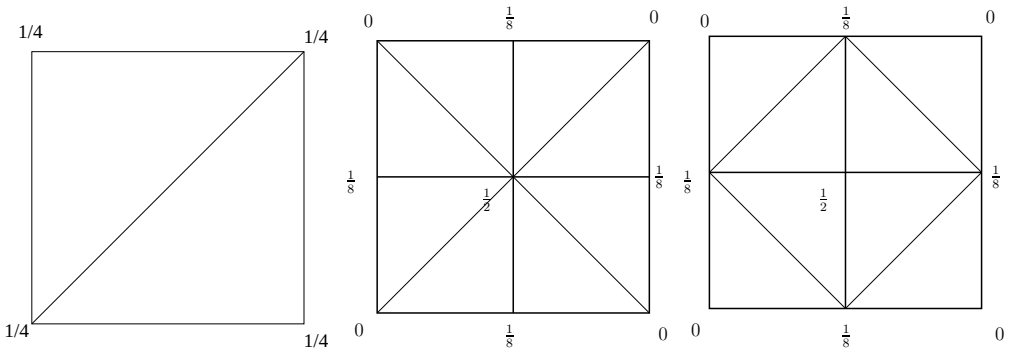

Figure 3.5: Face and vertex masks (regular case).

2. Each refinement step converts existing vertices of valence 4 to vertices of valence 8 by a refinement step.

3. The valence of vertices of valence 8 is not changed by refinement.

As already mentioned, complete refinement of a regular 4-8 mesh needs two bisection steps, and a bisection step has two sub-bisection steps: splitting faces and forming basic blocks.

1. The first bisection step:

   (a) Split face: A new vertex is added at every *interior edge* of every *basic block*. The adjoining triangular faces are split into two surfaces by linking the vertex to the opposite vertex of the face.

   (b) Form basic block: Convert two triangles sharing an *exterior edge* to a *basic block*. We observe that we can find which *interior edges* at the previous sub-step become *exterior edges*, and *exterior edges* at the previous sub-step which become *interior edges* at this step.

2. The second bisection step: Repeat the first bisection step.

Now we can obtain the local subdivision matrix using the method described in [26, Sec. 3.3] of the 4-8 subdivision scheme. Because the 4-8 subdivision scheme has two sub-steps, we have also two local subdivision matrices corresponding respectively to two sub-steps of refinement (the numbering of the rows of the matrix corresponds to the number indexing of the figures). The rows and columns are labelled here as in Figure 3.6 (a).

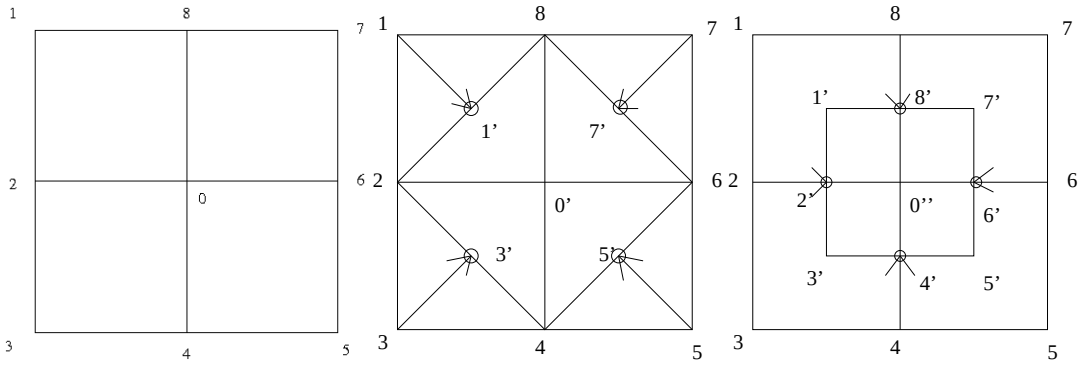

(a) A basic block (b) Sub-step1 (c) Sub-step2

Figure 3.6: 4-8 subdivision.

From sub-step 1 of the regular case of the 4-8 subdivision scheme, we have

$$\tilde{S}_1 = \frac{1}{8}\begin{pmatrix} 4 & 0 & 1 & 0 & 1 & 0 & 1 & 0 & 1 \\ 2 & 2 & 2 & 0 & 0 & 0 & 0 & 0 & 2 \\ 0 & 0 & 8 & 0 & 0 & 0 & 0 & 0 & 0 \\ 2 & 0 & 2 & 2 & 2 & 0 & 0 & 0 & 0 \\ 0 & 0 & 0 & 0 & 8 & 0 & 0 & 0 & 0 \\ 2 & 0 & 0 & 0 & 2 & 2 & 2 & 0 & 0 \\ 0 & 0 & 0 & 0 & 0 & 0 & 8 & 0 & 0 \\ 2 & 0 & 0 & 0 & 0 & 0 & 2 & 2 & 2 \\ 0 & 0 & 0 & 0 & 0 & 0 & 0 & 0 & 8 \end{pmatrix}.$$

From sub-step 2 of the regular case of the 4-8 subdivision scheme, we have

$$\tilde{S}_2 = \frac{1}{8}\begin{pmatrix} 4 & 1 & 0 & 1 & 0 & 1 & 0 & 1 & 0 \\ 0 & 8 & 0 & 0 & 0 & 0 & 0 & 0 & 0 \\ 2 & 2 & 2 & 2 & 0 & 0 & 0 & 0 & 0 \\ 0 & 0 & 0 & 8 & 0 & 0 & 0 & 0 & 0 \\ 2 & 0 & 0 & 2 & 2 & 2 & 0 & 0 & 0 \\ 0 & 0 & 0 & 0 & 0 & 8 & 0 & 0 & 0 \\ 2 & 0 & 0 & 0 & 0 & 2 & 2 & 2 & 0 \\ 0 & 0 & 0 & 0 & 0 & 0 & 0 & 8 & 0 \\ 2 & 2 & 0 & 0 & 0 & 0 & 0 & 2 & 2 \end{pmatrix}.$$

Finally, we can get the local 4-8 subdivision matrix $\tilde{S}$ for the regular case $\tilde{S} = \tilde{S}_2\tilde{S}_1$

$$\tilde{S} = \frac{1}{32}\begin{pmatrix} 12 & 1 & 4 & 1 & 4 & 1 & 4 & 1 & 4 \\ 8 & 8 & 8 & 0 & 0 & 0 & 0 & 0 & 8 \\ 8 & 2 & 13 & 2 & 3 & 0 & 1 & 0 & 3 \\ 8 & 0 & 8 & 8 & 8 & 0 & 0 & 0 & 0 \\ 8 & 0 & 3 & 2 & 13 & 2 & 3 & 0 & 1 \\ 8 & 0 & 0 & 0 & 8 & 8 & 8 & 0 & 0 \\ 8 & 0 & 1 & 0 & 3 & 2 & 13 & 2 & 3 \\ 8 & 0 & 0 & 0 & 0 & 0 & 8 & 8 & 8 \\ 8 & 2 & 3 & 0 & 1 & 0 & 3 & 2 & 13 \end{pmatrix},$$

which can be decomposed into

$$\tilde{S} = V^{-1}DV$$

where

$$V^{-1} = \frac{1}{12}\begin{pmatrix} 12 & 0 & 0 & 0 & 0 & -12 & -3 & -12 & -3 \\ 12 & 28 & 0 & 0 & -21 & -40 & 18 & 16 & -10 \\ 12 & 0 & -7 & -21 & 0 & 9 & 4 & -5 & 4 \\ 12 & -28 & -14 & 0 & 21 & 16 & -10 & 16 & 18 \\ 12 & -28 & -7 & 21 & 0 & -5 & 4 & 9 & -10 \\ 12 & -28 & 0 & 0 & -21 & 16 & 18 & -40 & 46 \\ 12 & 0 & 7 & -21 & 0 & 9 & -10 & 23 & -10 \\ 12 & 28 & 14 & 0 & 21 & -40 & 49 & -40 & 18 \\ 12 & 28 & 7 & 21 & 0 & 23 & -10 & 9 & 4 \end{pmatrix},$$

$$D = \frac{1}{8}\begin{pmatrix} 8 & 0 & 0 & 0 & 0 & 0 & 0 & 0 & 0 \\ 0 & 4 & 0 & 0 & 0 & 0 & 0 & 0 & 0 \\ 0 & 0 & 4 & 0 & 0 & 0 & 0 & 0 & 0 \\ 0 & 0 & 0 & 2 & 0 & 0 & 0 & 0 & 0 \\ 0 & 0 & 0 & 0 & 2 & 0 & 0 & 0 & 0 \\ 0 & 0 & 0 & 0 & 0 & 1 & 0 & 0 & 0 \\ 0 & 0 & 0 & 0 & 0 & 0 & 1 & 0 & 0 \\ 0 & 0 & 0 & 0 & 0 & 0 & 0 & 1 & 0 \\ 0 & 0 & 0 & 0 & 0 & 0 & 0 & 0 & 1 \end{pmatrix},$$

$$V = \frac{1}{28}\begin{pmatrix} 8 & 1 & 4 & 1 & 4 & 1 & 4 & 1 & 4 \\ 0 & 2 & 4 & 0 & -4 & -2 & -4 & 0 & 4 \\ 0 & -4 & -16 & -4 & 0 & 4 & 16 & 4 & 0 \\ 0 & 0 & -4 & 0 & 4 & 0 & -4 & 0 & 4 \\ 0 & -4 & 0 & 4 & 0 & -4 & 0 & 4 & 0 \\ -8 & -4 & 8 & -4 & 4 & 0 & 0 & 0 & 4 \\ -16 & 0 & 8 & -4 & 8 & 0 & 0 & 4 & 0 \\ -8 & 4 & -4 & 4 & 0 & 0 & 4 & 0 & 0 \\ 0 & 4 & -8 & 8 & -8 & 4 & 0 & 0 & 0 \end{pmatrix}.$$

We suppose $a_{i,j}$ is an entry of the matrices $\tilde{S}_1, \tilde{S}_2$ and $\tilde{S}$. The subscript ranges (i, j) of these matrices are from 0 to 9. The entries of the row_i represent the weights of subdivision mask applied to v_i and the j's entry of the row_i indicates this entry (weight) connected to v_j (see Figure 3.6).

The first row of the matrix V is the left eigenvector that will be used as the mask to compute the vertex's limit position of 4-8 subdivision scheme without iterative refinement steps. It is used below to parametrize the subdivision surfaces.

Chapter 4

Parametrization of Subdivision Surfaces

In [24], Wu and Peters introduced a new bound on maximum distance of the subdivision surfaces between the limit surface and its linear approximation. The bound can be computed locally and efficiently. The method of Wu-Peters is used for Loop's subdivision scheme [18]. In this thesis we apply the idea of Wu-Peters to parametrize Catmull-Clark and 4-8 subdivision surfaces and show how to compute linear approximations.

One problem related to subdivision surfaces is that of finding an explicit description for the limit surface. It is useful to be able to evaluate these surfaces directly, by parameterizing them, without explicitly subdividing. There are several methods allowing us to do this. For example, as already described above, Stam [21] evaluated and parametrized the subdivision surfaces in terms of a set of *eigenbasis* functions which depend on the subdivision scheme and these *eigenbasis* functions can be derived by eigendecomposition.

In our project, we use an alternate method developed in [17, 24, 25] to parametrize Catmull-Clark and 4-8 subdivision surfaces.

4.1 Parametrization of Catmull-Clark Subdivision Surfaces

In this section, we discuss the (u,v)-parametrization of the Catmull-Clark surface patches and compare two kinds of (u,v)-parametrizations: uniform parametrization and exact parametrizations.

We begin by discussing the parametrization of Catmull-Clark subdivision surfaces based on Catmull-Clark patches. A Catmull-Clark patch is a piece of the limit surface under Catmull-Clark subdivision applied to the quadrilateral and its one-ring neighbors. If each of the vertices of the quadrilateral has valence $n = 4$, it is called a regular patch. Otherwise, it is irregular. A Catmull-Clark patch has at most one extraordinary vertex which has $n \neq 4$ neighbors, since we assume that the initial mesh has been subdivided at least once, isolating the extraordinary vertices so that each Catmull-Clark patch contains at most one extraordinary vertex. We also assume that if a Catmull-Clark patch is irregular, the extraordinary vertex corresponds to the origin of the parametric domain of the patch.

In analogy with the development in [24, 25], we now derive parametrization for the Catmull-Clark method. We begin with a parametrization designed to be exact.

4.1.1 Exact Parametrization of Catmull-Clark Subdivision Surfaces

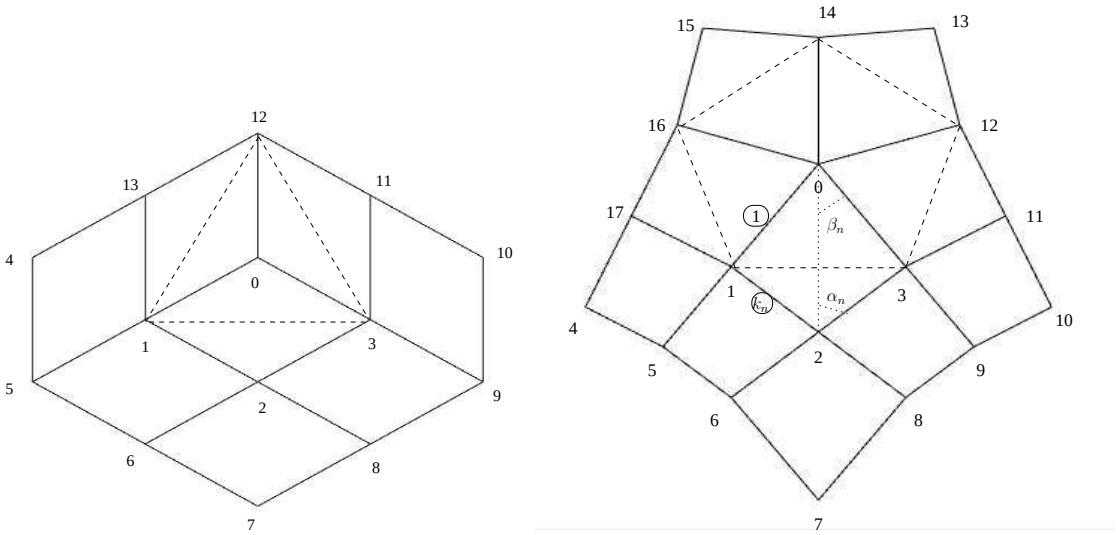

(a) valence n= 3

(b) valence n= 5

Figure 4.1: Parametrization around an extraordinary vertex.

We follow [24, 25] in replacing v_i by i in the figures below. To avoid confusion, lengths of edges are enclosed in circles in the figures.

To find a so-called exact parametrization for a patch adjacent to an extraordinary

vertex we propose the following construction (see Figure 4.1):

1. Set $v_0 = 0$, the origin of the (u, v) plane.
2. The direct neighbors $v_1, v_3, v_{12}, ..., v_{2n+6}$ of v_0 form a regular unit n-gon.
3. Define the angle formed by v_0 and two direct edges e_i and e_{i+1} of the n-gon as $2\alpha_n$ ($\alpha_n = \pi/n$).
4. Define the angle which is diagonal to $2\alpha_n$ as $2\beta_n$. The angle β_n is to be determined below.
5. Define the length of the edge between v_0 and direct neighbors of v_0 to be 1.
6. Define the length of other edges of the quadrilaterals of the one-ring neighborhood of v_0 to be k_n. The length of k_n is fixed by the choice of β_n and this fixes the values of $v_2, v_{11}, ..., v_{2n+7}$.
7. Define the $v_2, v_{11}, ..., v_{2n+7}$ using α_n, β_n, and k_n.
8. Extend the edges $v_{11}v_{12}$ and $v_{16}v_{17}$ by k_n to get v_{10} and v_4.
9. Extend the edges v_0v_1 and v_0v_3 by k_n to get v_5 and v_9.
10. Extend the edges v_1v_2 and v_3v_2 by k_n to get v_8 and v_6.
11. Extend the vertex v_2 in the direction of v_0v_2 by the length between v_0 and v_2 to get v_7.

With this kind of the parametrization, the vertices of v_0, v_1, v_2, and v_3 of Catmull-Clark patches are fixed (their original positions are equal to their limit positions) as will be shown below.

The angle β_n is defined by the following formula:

$$\beta_n = \begin{cases} \alpha_n & \text{if } n \leq 4 \\ \arcsin\left(bc + \dfrac{\sqrt{a^4 + a^2b^2 - a^2c^2}}{a^2 + b^2}\right) & \text{if } n > 4 \end{cases}$$

where

$$\begin{aligned} a &= -3\sin(\alpha_n)\cos(\alpha_n), \\ b &= 4 + 3\cos^2(\alpha_n), \\ c &= \sin(\alpha_n). \end{aligned}$$

The constant k_n is defined by the following formula:

$$k_n = \begin{cases} 1 & \text{if } n \leq 4 \\ \frac{\sin(\alpha_n)}{\sin(\beta_n)} & \text{if } n > 4 \end{cases}$$

The choice of a, b, and c is explained below.

We find that $k_n < 1$ and $\alpha_n < \beta_n < \frac{\pi}{2}$ when $n > 4$.

4.1.2 Uniform Parametrization of Catmull-Clark Subdivision Surfaces

To show the advantages of the exact parameterization, we compare it with the simpler uniform parameterization, described here.

Using the same construction as the exact parametrization, but with $k_n = 1$ and $\beta_n = \alpha_n$, we have the uniform parametrization. With the uniform parametrization, we have a big problem: when $n > 4$, the domain of the patch pushes out of the center quadrilateral (see Figures 4.2 and 4.3).

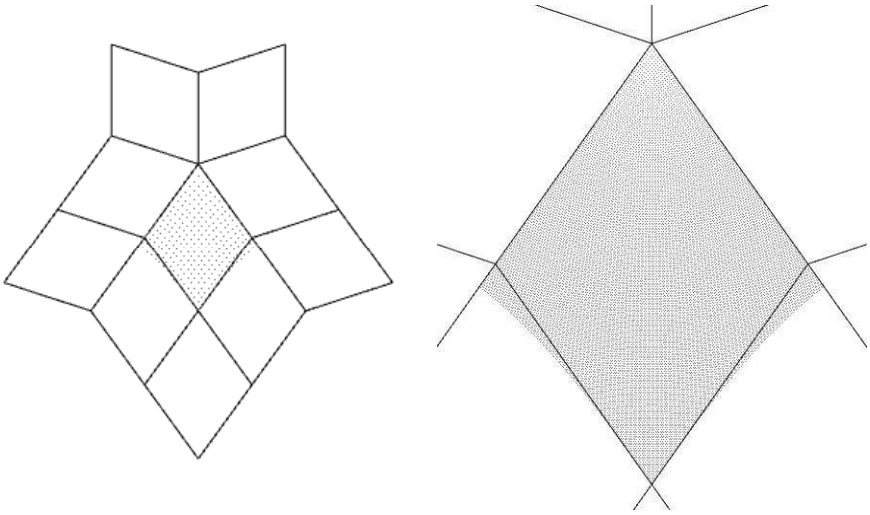

Figure 4.2: The domain (shaded area) of the uniform parametrization with $n = 5$.

Since the bounding volume is parametrized over the center quadrilateral, the bound is only safe if the patch domain lies inside the center quadrilateral. With the uniform parametrization, we can not bound the subdivision surfaces safely. We will show below that this problem is resolved by the exact parametrization.

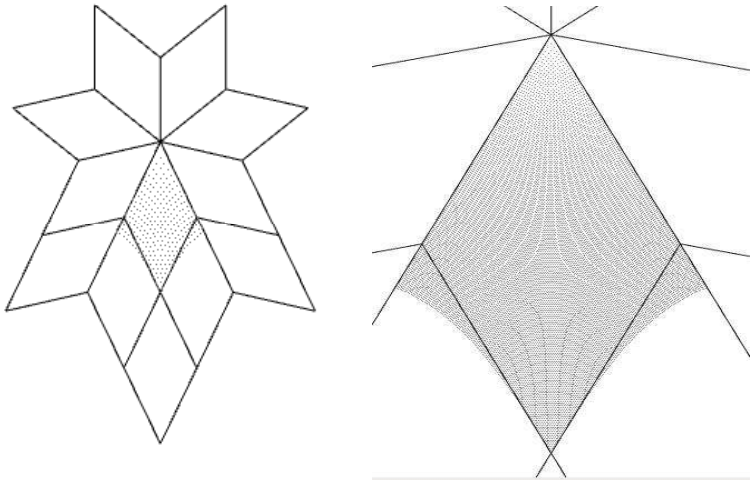

Figure 4.3: The domain (shaded area) of the uniform parametrization with $n = 7$.

4.1.3 Regular Vertex Limit Position Mask of Catmull-Clark Scheme

The uniform parametrization may not provide guaranteed bounding envelopes for surface patches when $n > 4$. So we should find a method to fix the value of β_n to envelop the patch domain within the center quadrilateral. To do this, we will choose β_n (and therefore k_n, v_2, v_{12}, etc.), so that the limit positions of v_1 and v_3 are equal to their original positions. The same will be true for v_0 and v_2.

To ensure that the limit positions of v_1 and v_3 are equal to their original positions, we compute the limit positions directly from the control points p_i^m on some level m without going through the iterative refinement. The standard technique in the analysis of subdivision schemes is:

1. Construct a local subdivision matrix.

2. Transform the local subdivision matrix into a basis of eigenvectors.

The Catmull-Clark subdivision scheme generalizes the bi-cubic B-spline surfaces of arbitrary topological type. The local support of the refinement rules for bi-cubic B-spline implies that the one-ring neighborhood of a vertex p^{m+1} only depends on the one-ring neighborhood of p^m. From the previous section, we have the local subdivision matrix of Catmull-Clark for the regular case (in our case, v_1 and v_3 are regular vertices):

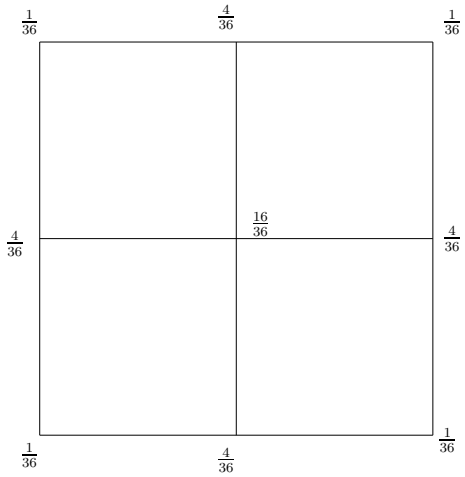

Figure 4.4: Limit position mask of regular vertex of the Catmull-Clark subdivision.

$$\tilde{S} = \frac{1}{64}\begin{pmatrix} 36 & 6 & 6 & 6 & 6 & 1 & 1 & 1 & 1 \\ 24 & 24 & 4 & 0 & 4 & 4 & 0 & 0 & 4 \\ 24 & 4 & 24 & 4 & 0 & 4 & 4 & 0 & 0 \\ 24 & 0 & 4 & 24 & 4 & 0 & 4 & 4 & 0 \\ 24 & 4 & 0 & 4 & 24 & 0 & 0 & 4 & 4 \\ 16 & 16 & 16 & 0 & 0 & 16 & 0 & 0 & 0 \\ 16 & 0 & 16 & 16 & 0 & 0 & 16 & 0 & 0 \\ 16 & 0 & 0 & 16 & 16 & 0 & 0 & 16 & 0 \\ 16 & 16 & 0 & 0 & 16 & 0 & 0 & 0 & 16 \end{pmatrix},$$

which can be decomposed into $\tilde{S} = V^{-1}DV$, where

$$V^{-1} = \begin{pmatrix} 1 & 0 & 0 & -2 & -2 & -2 & 0 & 0 & 1 \\ 1 & 3 & -3 & 1 & 1 & -8 & -3 & 3 & -2 \\ 1 & -3 & -3 & 1 & 1 & 10 & 3 & 3 & -2 \\ 1 & -3 & 3 & 1 & 1 & -8 & 3 & -3 & -2 \\ 1 & 3 & 3 & 1 & 1 & 10 & -3 & -3 & -2 \\ 1 & 0-6 & -5 & 13 & 4 & 0 & -12 & 4 & \\ 1 & -6 & 0 & 13 & -5 & 4 & -12 & 0 & 4 \\ 1 & 0 & 6 & -5 & 13 & 4 & 0 & 12 & 4 \\ 1 & 6 & 0 & 13 & -5 & -4 & 12 & 0 & 4 \end{pmatrix},$$

$$D = \frac{1}{16}\begin{pmatrix} 16 & 0 & 0 & 0 & 0 & 0 & 0 & 0 & 0 \\ 0 & 8 & 0 & 0 & 0 & 0 & 0 & 0 & 0 \\ 0 & 0 & 8 & 0 & 0 & 0 & 0 & 0 & 0 \\ 0 & 0 & 0 & 4 & 0 & 0 & 0 & 0 & 0 \\ 0 & 0 & 0 & 0 & 4 & 0 & 0 & 0 & 0 \\ 0 & 0 & 0 & 0 & 0 & 4 & 0 & 0 & 0 \\ 0 & 0 & 0 & 0 & 0 & 0 & 2 & 0 & 0 \\ 0 & 0 & 0 & 0 & 0 & 0 & 0 & 2 & 0 \\ 0 & 0 & 0 & 0 & 0 & 0 & 0 & 0 & 1 \end{pmatrix},$$

$$V = \frac{1}{36}\begin{pmatrix} 16 & 4 & 4 & 4 & 4 & 1 & 1 & 1 & 1 \\ 0 & 2 & -2 & -2 & 2 & 0 & -1 & 0 & 1 \\ 0 & -2 & -2 & 2 & 2 & -1 & 0 & 1 & 0 \\ -4 & 1 & 0 & 1 & 0 & 0 & 1 & 0 & 1 \\ -4 & 1 & 0 & 1 & 0 & 1 & 0 & 1 & 0 \\ 0 & -1 & 1 & -1 & 1 & 0 & 0 & 0 & 0 \\ 0 & -1 & 1 & 1 & -1 & 0 & -1 & 0 & 1 \\ 0 & 1 & 1 & -1 & -1 & -1 & 0 & 1 & 0 \\ 4 & -2 & -2 & -2 & -2 & 1 & 1 & 1 & 1 \end{pmatrix}.$$

From the above analysis of the local subdivision matrix (this decomposition was done by using Mathematica), we know that the Catmull-Clark subdivision scheme has eigenvalues

$$(\lambda_0, \lambda_1, \lambda_2, \lambda_3, \lambda_4, \lambda_5, \lambda_6, \lambda_7, \lambda_8) = \left(1, \frac{1}{2}, \frac{1}{2}, \frac{1}{4}, \frac{1}{4}, \frac{1}{4}, \frac{1}{8}, \frac{1}{8}, \frac{1}{16}\right).$$

We now have the regular vertex limit position mask [2, Sec. 5.4]:

$$\left(\frac{16}{36}, \frac{4}{36}, \frac{4}{36}, \frac{4}{36}, \frac{4}{36}, \frac{1}{36}, \frac{1}{36}, \frac{1}{36}, \frac{1}{36}\right).$$

With this mask, we can compute a regular vertex's limit position directly considering the one-ring neighborhood of the vertex. The ability to compute the regular vertex's limit position directly is important in the phase of the exact parametrization of Catmull-Clark subdivision surfaces.

4.1.4 Computation of Exact Parametrization of Catmull-Clark Surfaces

Having the limit position mask for regular vertex of the Catmull-Clark subdivision scheme, we can compute the parameters of exact parametrization for the Catmull-Clark subdivision scheme. To envelop the limit surface of one Catmull-Clark patch, we need to consider the v_0, v_1, v_2, v_3 and from the limit position mask we know that we just need one-ring neighborhood of the vertex to compute the limit position. The limit positions of the v_0 and v_2 are always equal to their original positions by the central symmetry of their one-ring neighborhood. For v_1 and v_3, we should adjust their one-ring neighbors' positions to assure their limit positions are equal to their original positions if the valence of v_0 is $n > 4$.

We use the patch of valence $n = 5$ to illustrate. First, we consider v_1; the one-ring neighbors of v_1 are $v_0, v_2, v_3, v_4, v_5, v_6, v_{16}$, and v_{17}.

To fix v_1, we have the following formula by the limit position mask:

$$v_1 = \frac{16}{36}v_1 + \frac{4}{36}(v_0 + v_{17} + v_5 + v_2) + \frac{1}{36}(v_3 + v_{16} + v_4 + v_6). \tag{4.1}$$

For easier computation, we rotate the planar grid by α_n. It is clear by symmetry that the horizontal components in the new coordinate system of the average of the one-ring neighbors of v_1 does not affect the horizontal component of v_1. So we just consider the vertical components.

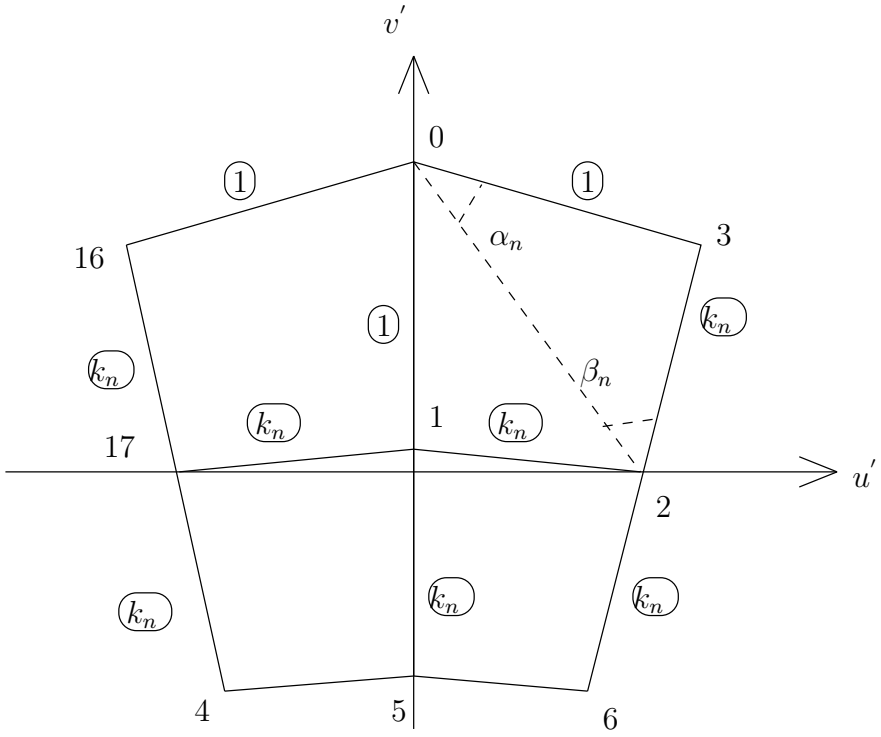

Figure 4.5: Control points for Catmull-Clark patch with $n = 5$.

The vertical component (positive downwards) of each relevant vertex is:

$$v_0 = 0 \tag{4.2}$$

$$v_1 = 1 \tag{4.3}$$

$$v_3 = v_{16} \tag{4.4}$$

$$v_2 = v_{17} \tag{4.5}$$

$$v_4 = v_6 = v_2 + (v_2 - v_3) = 2v_2 - v_3. \tag{4.6}$$

From Equation (4.1), we have

$$v_1 = \frac{16}{36}v_1 + \frac{4}{36}(v_0 + v_{17} + v_5 + v_2) + \frac{1}{36}(v_3 + v_{16} + v_4 + v_6) \tag{4.7}$$

$$\implies \frac{5}{9}v_1 = \frac{1}{9}(2v_2 + v_5) + \frac{1}{36}(2v_4 + 2v_3) \tag{4.8}$$

$$\implies 10v_1 = 4v_2 + 2v_5 + v_6 + v_3 \tag{4.9}$$

$$\implies 5v_1 = 3v_2 + v_5 \tag{4.10}$$

where the vertical components of vertices are

$$v_1 = 1 \tag{4.11}$$

$$v_2 = -\frac{\sin(\alpha_n + \beta_n)}{\sin\beta_n}\cos\alpha_n \tag{4.12}$$

$$v_5 = 1 + \frac{\sin\alpha_n}{\sin\beta_n}. \tag{4.13}$$

Equations (4.12) and (4.13) follow immediately from the law of sines.

With Equations (4.11), (4.12) and (4.13), we transform the vertical component of Equation (4.10) into

$$\frac{-3\sin(\alpha_n + \beta_n)\cos\alpha_n}{\sin\beta_n} + \frac{\sin\alpha_n}{\sin\beta_n} = 4 \tag{4.14}$$

$$\implies -3\sin(\alpha_n + \beta_n)\cos\alpha_n + \sin\alpha_n = 4\sin\beta_n \tag{4.15}$$

$$\implies -3\sin\alpha_n\cos\alpha_n\cos\beta_n - \sin\beta_n(4 + 3\cos^2\alpha_n) + \sin\alpha_n = 0. \tag{4.16}$$

In Equation (4.16), we set

$$a = -3\sin\alpha_n\cos\alpha_n \tag{4.17}$$

$$b = 4 + 3\cos^2\alpha_n \tag{4.18}$$

$$c = \sin\alpha_n. \tag{4.19}$$

With Equations (4.17), (4.18), and (4.19), we can transform Equation (4.16) into

$$a\sqrt{1 - \sin^2\beta_n} - b\sin\beta_n + c = 0 \tag{4.20}$$

$$\implies \left(a^2 + b^2\right)\sin^2\beta_n - 2bc\sin\beta + c^2 - a^2 = 0 \tag{4.21}$$

From Equation (4.21), we have the solutions

$$\sin\beta_n = \frac{bc \pm \sqrt{a^4 + a^2b^2 - a^2c^2}}{a^2 + b^2}. \tag{4.22}$$

Since $0 < \beta_n < \frac{\pi}{2}$, we have the unique result

$$\sin\beta_n = \frac{bc + \sqrt{a^4 + a^2b^2 - a^2c^2}}{a^2 + b^2}. \tag{4.23}$$

$$\implies \beta_n = \arcsin\left(\frac{bc + \sqrt{a^4 + a^2b^2 - a^2c^2}}{a^2 + b^2}\right) \tag{4.24}$$

where

$$\begin{aligned} \alpha_n &= \tfrac{\pi}{n} \\ a &= -3\sin\alpha_n\cos\alpha_n \\ b &= 4 + 3\cos^2\alpha_n \\ c &= \sin\alpha_n. \end{aligned}$$

With this kind of parametrization, we see empirically that the domain the Catmull-Clark patch is strictly within the center quadrilateral (cf. Figures 4.2 and 4.3).

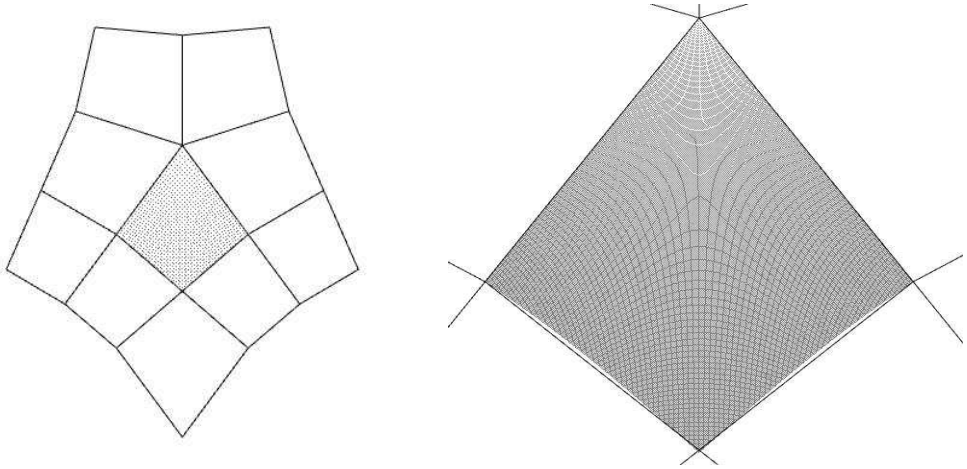

Figure 4.6: The domain (shaded area) of the exact parametrization of the Catmull-Clark patch with $n = 5$.

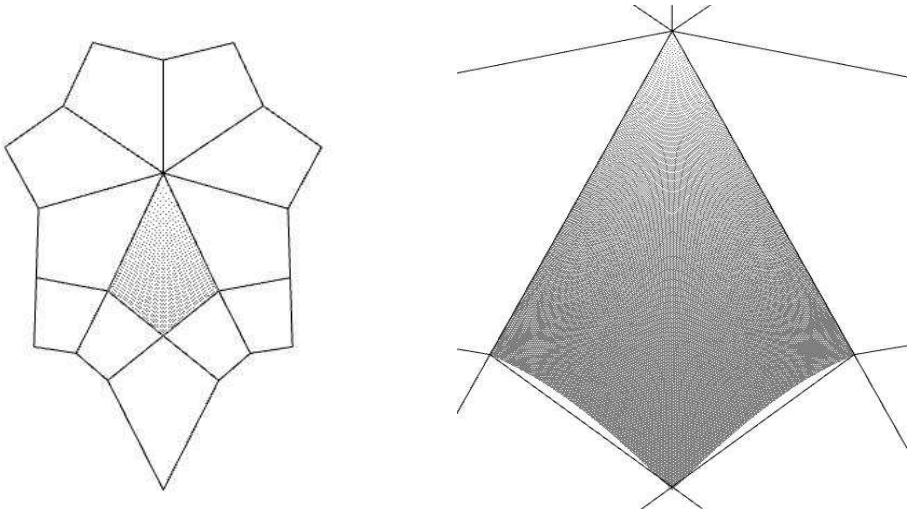

Figure 4.7: The domain (shaded area) of the exact parametrization of the Catmull-Clark patch with $n = 7$.

We have observed the domains of the Catmull-Clark patches with valence up to 15 are strictly within the center quadrilaterals. The domain Ω_n of the Catmull-Clark patch is the limit of the subdivision applied to the initial mesh of the abscissae v_i [2, Sec. 6.5]. We choose the abscissae mesh to be symmetric with respect to the extraordinary node. The Ω_n falls into the sector formed by the initial abscissa quadrilateral with vertices v_0, v_1, v_2, and v_3 (see Figure 4.1).

We note with satisfaction that the domains are visually close to the quadrilaterals. Thus the bounds will be safe and realistic. It would be interesting to quantify the discrepancy referred to by the word "close", but it would not be trivial to give an exact value for the maximum value of this discrepancy. A more practical approach would be to examine empirically the consequences of the discrepancy in model space R^3.

4.2 Parametrization of 4-8 Subdivision Surfaces

In this section, we discuss the (u, v)-parametrization of 4-8 subdivision surfaces and again compare two kinds of (u, v)-parametrizations: uniform and exact parametrizations.

Compared to the parametrization of the Catmull-Clark subdivision surfaces, the parametrization of the 4-8 subdivision surfaces is more complex. We know that a Catmull-Clark patch is a piece of the limit surface under Catmull-Clark subdivision

applied to the quadrilateral and its one-ring neighbors. But a 4-8 patch is a piece of the limit surface under 4-8 subdivision applied to the quadrilateral and its two-ring neighbors (see Figure 4.8). Because there are more one-ring neighbors than for a Catmull-Clark patch, the parametrization of the 4-8 subdivision surfaces becomes more complex.

For the Catmull-Clark subdivision scheme, after one local subdivision, we may assume that a Catmull-Clark patch has at most one extraordinary vertex and we can assume if a Catmull-Clark patch has an extraordinary vertex, this vertex is the origin by transforming the patch by a rigid motion. But this is not true for the 4-8 subdivision scheme:

1. The 4-8 subdivision scheme needs two complete subdivision steps to ensure that each 4-8 patch has at most one extraordinary vertex.

2. Even if we can assure that a 4-8 patch has at most one extraordinary vertex, we cannot assure that the extraordinary vertex belongs to the center quadrilateral (see Figures 4.9, 4.10, and 4.11).

Fortunately, we can guarantee that there are only two situations for a 4-8 patch's extraordinary vertex:

1. It belongs to the center quadrilateral.

2. It belongs to the one-ring neighbors of the center quadrilateral.

We can classify all situations into four categories:

1. Category I: Each vertex of the patch is regular or v_0 is an extraordinary vertex (see Figure 4.8).

2. Category II: Extraordinary vertex is v_4 (see Figure 4.9).

3. Category III: Extraordinary vertex is v_{15} (see Figure 4.10).

4. Category IV: Extraordinary vertex is v_5 (see Figure 4.11).

If an extraordinary vertex belonging to the center quadrilateral is not v_0 or an extraordinary vertex belonging to the one-ring neighbors of v_0 are not v_4, v_5, or v_{15}, we can rotate the coordinate domain to obtain one of the four categories we defined here.

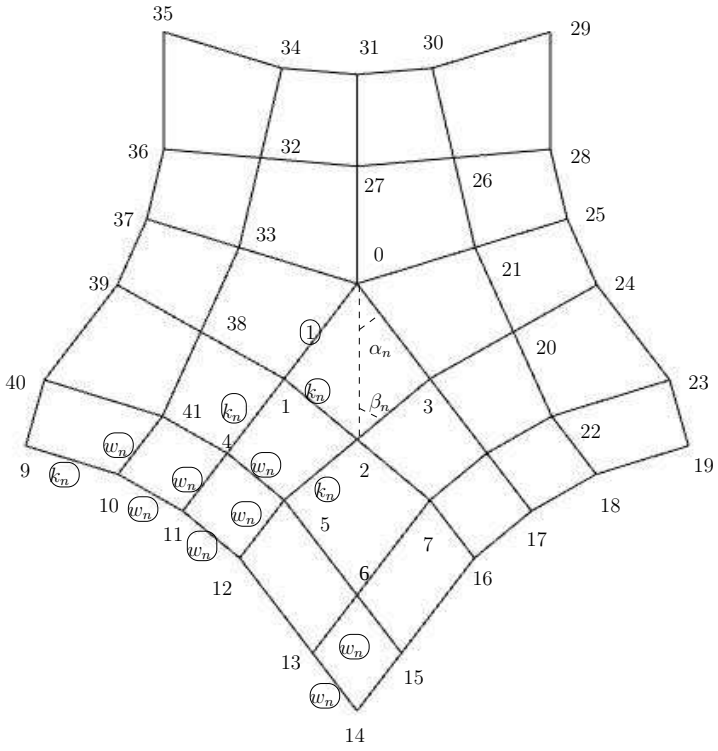

Figure 4.8: Parametrization of 4-8 patch (n=5): Category I.

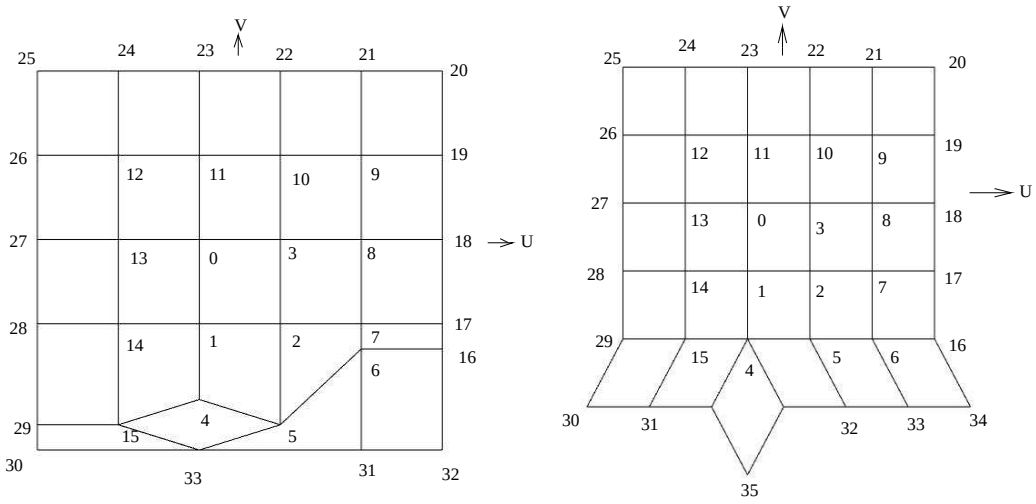

(a) n=3 (b) n=5

Figure 4.9: Parametrization of 4-8 patch: Category II.

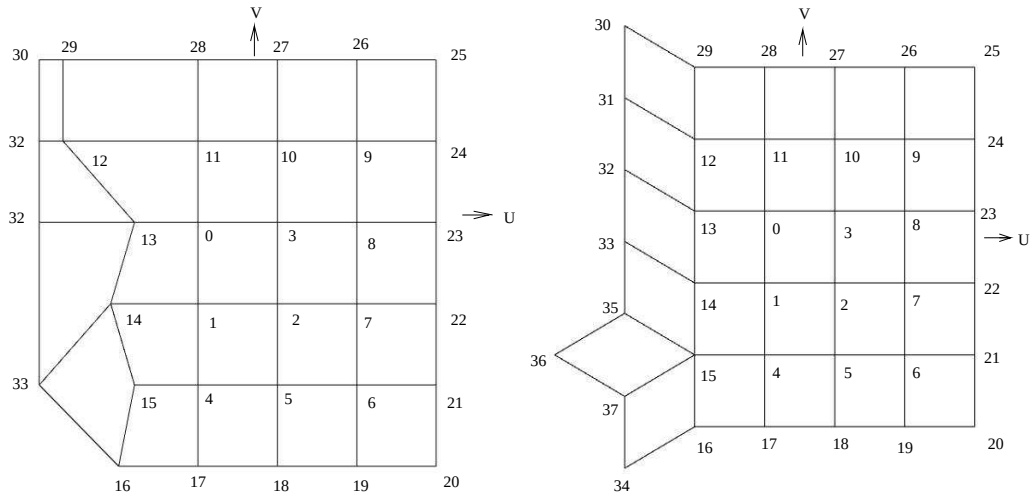

(a) n =3 (b) n =5

Figure 4.10: Parametrization of 4-8 patch: Category III.

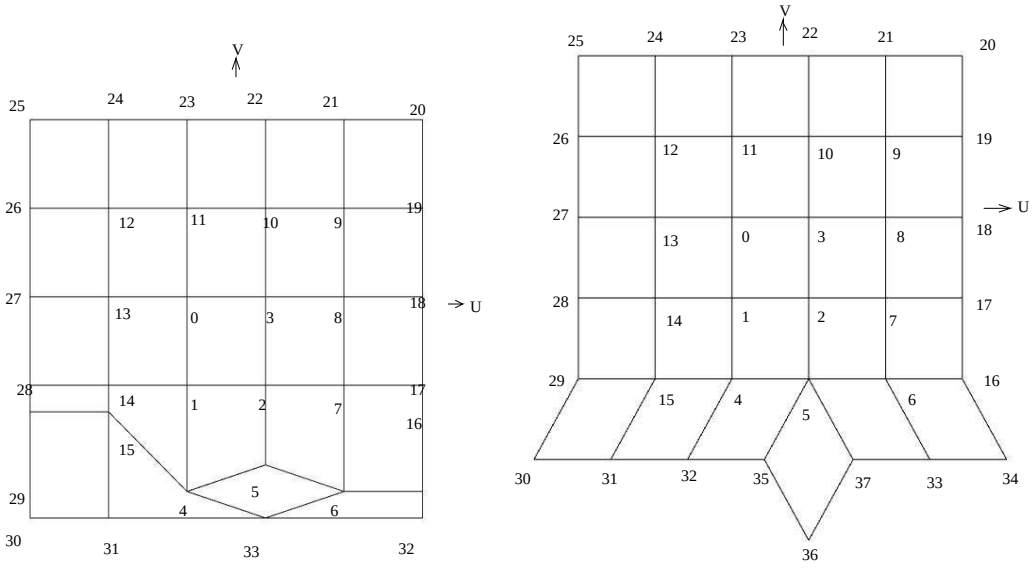

(a) n =3 (b) n =5

Figure 4.11: Parametrization of 4-8 patch: Category IV.

4.2.1 Exact Parametrization of 4-8 Surfaces (Category I)

The parametrization of Category I is defined by the following construction (Figure 4.8 illustrates the case $n = 5$). The construction is similar to the one used for the Catmull-

Clark scheme:

1. Set $v_0 = 0$, the origin of the (u, v) plane.

2. The n quadrilaterals around v_0 form a one-ring neighborhood of v_0. Define the angles formed by v_0 and two consecutive direct neighbors v_i and v_{i+1} as $2\alpha_n$. Define the angle which is diagonal to $2\alpha_n$ as $2\beta_n$ (β_n is to be determined in Sec. 4.2.4 (see Equation (4.35))). The length of the edges between v_0 and direct neighbors of v_0 is defined to be 1. Define the length of the other edges of the one-ring neighborhood of v_0 to be k_n. The value of k_n is fixed by the choice of β_n.

3. Define the two-ring neighborhood of v_0. The two-ring neighborhood of v_0 can be divided into n sectors (n is the valence of v_0):

   (a) Define the first sector of the two-ring neighborhood of v_0:

      i. Extend the edges v_0v_1 and v_0v_3 by k_n to get v_4 and v_8.

      ii. Extend the edges v_2v_3 and v_1v_2 by k_n to get v_5 and v_7.

      iii. Choose v_6 at distance v_0v_2 from v_2 in the direction of v_0v_2 to get v_6.

   (b) Use the same rules as those defining v_5, v_6, v_7, and v_8 of the first sector for the corresponding vertices of the other sectors of the second-ring neighborhood of v_0 (the vertex in each of the sectors which corresponds to v_4 of the first sector has in each case been defined in the previous sector. Thus, there are two vertices of the final sector that have been defined in the first sector and the sector $n - 1$).

4. The parametrization of vertices can now be fixed whatever the valence of v_0:

   (a) Extend the edges v_1v_4 and v_3v_8 by w_n to get v_{11} and v_{17}. The value of w_n is given below; it is fixed by the choice of β_n.

   (b) Add an edge of length w_n from the vertex v_{11} parallel to the direction of v_4v_5 to get v_{12}.

   (c) Add an edge of length w_n from the vertex v_{17} parallel to the direction of v_7v_8 to get v_{16}.

   (d) Extend the edge $v_{11}v_{12}$ by k_n to get v_{13}. Make the edge $v_{12}v_{13}$ parallel to the edge v_5v_6.

(e) Extend the edge $v_{16}v_{17}$ by k_n to get v_{15}. Make the edge $v_{15}v_{16}$ parallel to the edge v_6v_7.

(f) Extend the edge $v_{12}v_{13}$ by w_n to get v_{14}. Make the edge $v_{13}v_{14}$ parallel to the edge v_6v_{15}.

(g) Add an edge from the vertex v_{11} in the direction of v_4v_{41} by w_n to get v_{10}. Make the edge $v_{10}v_{11}$ parallel to the edge v_4v_{41}.

(h) Add an edge from the vertex v_{17} in the direction v_8v_{22} by w_n to get v_{18}. Make the edge $v_{17}v_{18}$ parallel to the edge v_8v_{22}.

(i) Extend the edge $v_{10}v_{11}$ by k_n to get v_9. Make the edge v_9v_{10} parallel to the edge $v_{40}v_{41}$.

(j) Extend the edge $v_{17}v_{18}$ by k_n to get the v_{19}. Make the edge $v_{18}v_{19}$ parallel to the edge $v_{22}v_{23}$.

With this kind of the parametrization, the vertices of v_0, v_1, v_2, and v_3 of 4-8 patches (category I) are fixed (their original positions are equal to their limit positions).

The angle β_n is defined by the following formula

$$\beta_n = \begin{cases} \alpha_n & \text{if } n \leq 4 \\ \arcsin\left(bc + \dfrac{\sqrt{a^4 + a^2b^2 - a^2c^2}}{a^2 + b^2}\right) & \text{if } n > 4 \end{cases}$$

where

$$\begin{aligned} a &= -3\sin(\alpha_n)\cos(\alpha_n) \\ b &= 4 + 3\cos^2(\alpha_n) \\ c &= \sin(\alpha_n). \end{aligned}$$

The choice of a, b, and c is explained below.

The constant k_n is defined by the following formula

$$k_n = \begin{cases} 1 & \text{if } n \leq 4 \\ \dfrac{\sin(\alpha_n)}{\sin(\beta_n)} & \text{if } n > 4 \end{cases}$$

where $\alpha_n = \frac{\pi}{n}$, and w_n is the length between v_4 and v_5 in the plane xy. We also have $\alpha_n < \beta_n < \frac{\pi}{2}$ and $k_n < 1$ when $n > 4$.

This choice of w_n was made on intuitive grounds. We have verified for valences up to $n = 25$ that this choice for w_n leads to a well-formed mesh [5] in the plane.

4.2.2 Uniform Parametrization of 4-8 Surfaces (Category I)

Again for purposes of comparison, we consider the simpler uniform parametrization. With the same construction as the exact parametrization, but $k_n = 1$, $\beta_n = \alpha_n$, we have the uniform parametrization (w_n will be automatically equal to 1). With the uniform parametrization, we have a big problem. When $n > 4$, the domain of the 4-8 patch pushes out of the center quadrilateral. This phenomenon is exactly as that of uniform parametrization of Catmull-Clark subdivision surfaces (see Sec. 4.1.2) and it recurs for the other categories of parametrization of 4-8 subdivision surfaces.

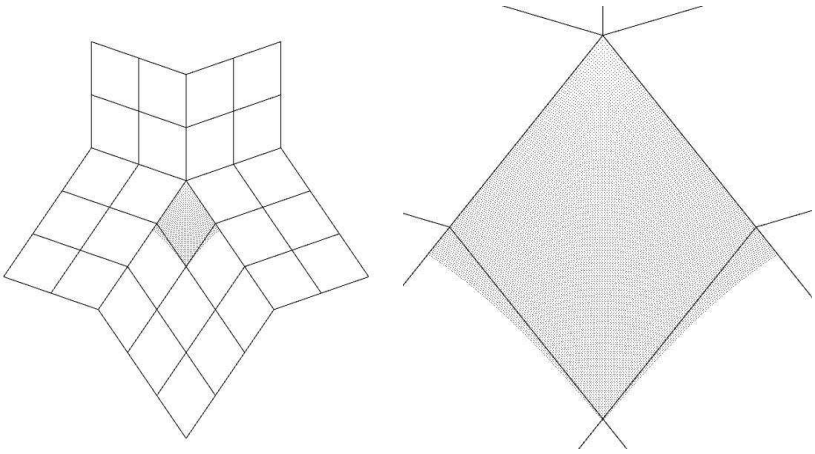

Figure 4.12: The domain (shaded area) of the uniform parametrization ($n = 5$).

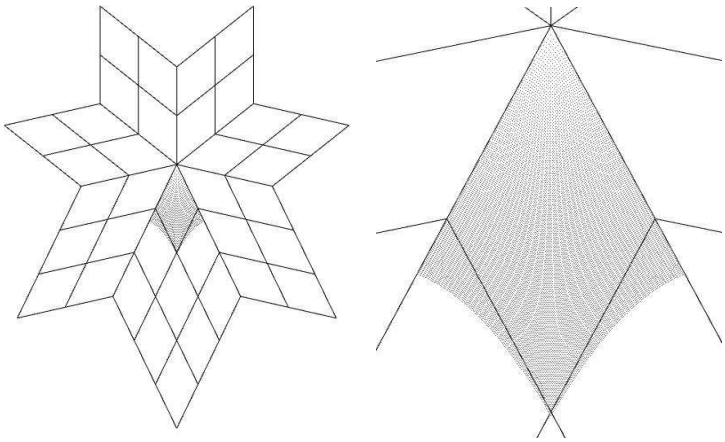

Figure 4.13: The domain (shaded area) of the uniform parametrization ($n = 7$).

4.2.3 Regular Vertex Limit Position Mask of 4-8 Scheme

We see that the uniform parametrization does not provide guaranteed bounding envelopes for surface patches when $n > 4$. We must find a solution to fix the value of β_n to envelop the limit surface within the center quadrilateral. To do this, we will choose β_n (and therefore k_n, w_n, etc.), so that the limit positions of v_1 and v_3 are equal to their original positions. The same will be true for v_0 and v_2.

To ensure that the limit position of v_1 or v_3 is equal to its original position, we compute the limit position directly from the control points p_i^m on some level m without going through the iterative refinement. We again use the standard technique in the analysis of subdivision schemes:

1. Construct a local subdivision matrix.

2. Transform the local subdivision matrix into a basis of eigenvectors.

The 4-8 subdivision scheme generalizes the four directional box splines of class C^4 to arbitrary locally-planar meshes. The local support of the refinement rules for four directional box splines imply that the corresponding patch only depends on the one-ring neighborhood of p^m. The limit positions of v_0 and v_2 are always equal to their original positions by the symmetry of their one-ring neighbors. We will also choose parameter values so that v_1 and v_3 are mapped into themselves by the subdivision process. In the previous section, we have the local subdivision matrix of the 4-8 subdivision scheme for the regular case (in our case, v_1 and v_3 are regular vertices) from which we can get the limit position mask of the regular vertex and we can compute the limit position of v_1 and v_3 directly.

We have the local 4-8 subdivision matrix $\tilde{S}$ from Section 3.2.2 for the regular vertex with valence 4:

$$\tilde{S} = \frac{1}{32}\begin{pmatrix} 12 & 1 & 4 & 1 & 4 & 1 & 4 & 1 & 4 \\ 8 & 8 & 8 & 0 & 0 & 0 & 0 & 0 & 8 \\ 8 & 2 & 13 & 2 & 3 & 0 & 1 & 0 & 3 \\ 8 & 0 & 8 & 8 & 8 & 0 & 0 & 0 & 0 \\ 8 & 0 & 3 & 2 & 13 & 2 & 3 & 0 & 1 \\ 8 & 0 & 0 & 0 & 8 & 8 & 8 & 0 & 0 \\ 8 & 0 & 1 & 0 & 3 & 2 & 13 & 2 & 3 \\ 8 & 0 & 0 & 0 & 0 & 0 & 8 & 8 & 8 \\ 8 & 2 & 3 & 0 & 1 & 0 & 3 & 2 & 13 \end{pmatrix},$$

which can be decomposed into

$$\tilde{S} = V^{-1}DV$$

where

$$V^{-1} = \frac{1}{12}\begin{pmatrix} 12 & 0 & 0 & 0 & 0 & -12 & -3 & -12 & -3 \\ 12 & 28 & 0 & 0 & -21 & -40 & 18 & 16 & -10 \\ 12 & 0 & -7 & -21 & 0 & 9 & 4 & -5 & 4 \\ 12 & -28 & -14 & 0 & 21 & 16 & -10 & 16 & 18 \\ 12 & -28 & -7 & 21 & 0 & -5 & 4 & 9 & -10 \\ 12 & -28 & 0 & 0 & -21 & 16 & 18 & -40 & 46 \\ 12 & 0 & 7 & -21 & 0 & 9 & -10 & 23 & -10 \\ 12 & 28 & 14 & 0 & 21 & -40 & 49 & -40 & 18 \\ 12 & 28 & 7 & 21 & 0 & 23 & -10 & 9 & 4 \end{pmatrix},$$

$$D = \frac{1}{8}\begin{pmatrix} 8 & 0 & 0 & 0 & 0 & 0 & 0 & 0 & 0 \\ 0 & 4 & 0 & 0 & 0 & 0 & 0 & 0 & 0 \\ 0 & 0 & 4 & 0 & 0 & 0 & 0 & 0 & 0 \\ 0 & 0 & 0 & 2 & 0 & 0 & 0 & 0 & 0 \\ 0 & 0 & 0 & 0 & 2 & 0 & 0 & 0 & 0 \\ 0 & 0 & 0 & 0 & 0 & 1 & 0 & 0 & 0 \\ 0 & 0 & 0 & 0 & 0 & 0 & 1 & 0 & 0 \\ 0 & 0 & 0 & 0 & 0 & 0 & 0 & 1 & 0 \\ 0 & 0 & 0 & 0 & 0 & 0 & 0 & 0 & 1 \end{pmatrix},$$

$$V = \frac{1}{28}\begin{pmatrix} 8 & 1 & 4 & 1 & 4 & 1 & 4 & 1 & 4 \\ 0 & 2 & 4 & 0 & -4 & -2 & -4 & 0 & 4 \\ 0 & -4 & -16 & -4 & 0 & 4 & 16 & 4 & 0 \\ 0 & 0 & -4 & 0 & 4 & 0 & -4 & 0 & 4 \\ 0 & -4 & 0 & 4 & 0 & -4 & 0 & 4 & 0 \\ -8 & -4 & 8 & -4 & 4 & 0 & 0 & 0 & 4 \\ -16 & 0 & 8 & -4 & 8 & 0 & 0 & 4 & 0 \\ -8 & 4 & -4 & 4 & 0 & 0 & 4 & 0 & 0 \\ 0 & 4 & -8 & 8 & -8 & 4 & 0 & 0 & 0 \end{pmatrix}.$$

From the above subdivision matrix analysis, we see that the 4-8 subdivision scheme has eigenvalues:

$$(\lambda_0, \lambda_1, \lambda_2, \lambda_3, \lambda_4, \lambda_5, \lambda_6, \lambda_7, \lambda_8) = \left(1, \frac{1}{2}, \frac{1}{2}, \frac{1}{4}, \frac{1}{4}, \frac{1}{8}, \frac{1}{8}, \frac{1}{8}, \frac{1}{8}\right).$$

We now have the regular vertex limit position mask (the mask is the first row of the matrix V) [2, Sec. 5.4]:

$$\left(\frac{8}{28}, \frac{1}{28}, \frac{4}{28}, \frac{1}{28}, \frac{4}{28}, \frac{1}{28}, \frac{4}{28}, \frac{1}{28}, \frac{4}{28}\right).$$

With this mask, we can compute a regular vertex's limit position directly just considering the one-ring neighborhood of the vertex. The ability to compute the regular vertex's limit position directly is important in the phase of the exact parametrization of 4-8 subdivision surfaces.

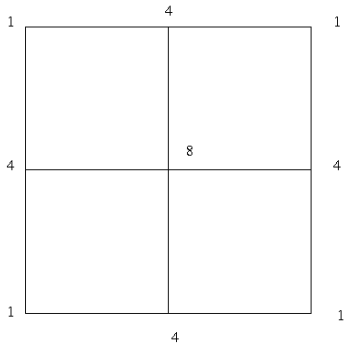

Figure 4.14: Regular vertex limit position mask for 4-8 subdivision scheme.

4.2.4 Computation of Exact Parametrization (Category I)

To envelop the limit surface, we just need to consider the vertices v_0, v_1, v_2, v_3 and from the limit position mask we know that we just need the one-ring neighborhood of the vertex to compute the limit position. These limit positions of v_0 and v_2 are always equal to their original positions by the symmetry of their one-ring neighborhood. For v_1 and v_3, we should adjust their one-ring neighbors' positions to assure their limit positions are equal to their original positions if the valence of v_0 is $n > 4$.

We use the patch of valence 5 to illustrate. First, we consider v_1: the neighbors of v_1 are $v_0, v_2, v_3, v_4, v_5, v_{6n+3}, v_{6n+8}$, and v_{6n+11}.

To fix v_1, we have the following formula from the limit position mask

$$\frac{8}{28}v_1 + \frac{4}{28}(v_0 + v_{6n+8} + v_4 + v_2) + \frac{1}{28}(v_{6n+3} + v_{6n+11} + v_5 + v_3) = v_1. \tag{4.25}$$

For easier computation, we rotate the planar patch by α_n; it is clear by symmetry that the horizontal components in the new coordinate system of the one-ring neighbors of v_1 and v_3 do not affect the horizontal component of v_1 and v_3. Consequently, we just consider the vertical components.

The vertical component (positive downwards) of

$$v_0 = 0 \tag{4.26}$$

$$v_1 = 1 \tag{4.27}$$

$$v_3 = v_{33} \tag{4.28}$$

$$v_2 = v_{38} \tag{4.29}$$

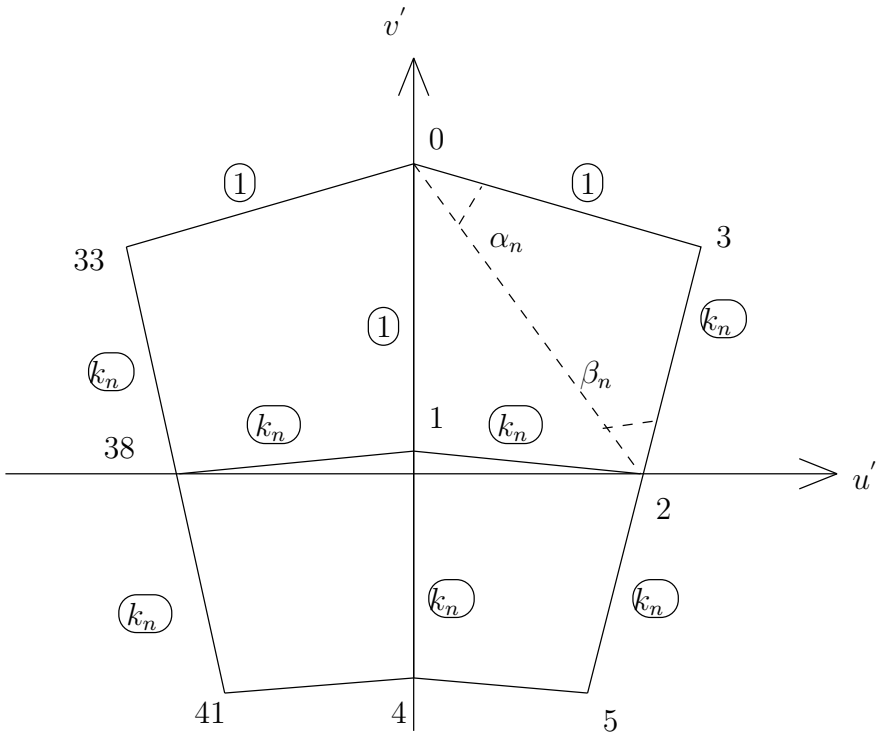

Figure 4.15: Control points for 4-8 patch.

$$v_5 = v_{41} = v_2 + (v_2 - v_3) = 2v_2 - v3. \tag{4.30}$$

With Equations (4.26), (4.27), (4.28), (4.29), and (4.30), we can reduce Equation (4.25) to

$$5v_1 = 2v_2 + v_4 \tag{4.31}$$

where the vertical component of

$$v_1 = 1 \tag{4.32}$$

$$v_2 = -\frac{\sin(\alpha_n + \beta_n)}{\sin \beta_n} \cos \alpha_n \tag{4.33}$$

$$v_4 = 1 + \frac{\sin \alpha_n}{\sin \beta_n}. \tag{4.34}$$

Equations (4.33) and (4.34) follow immediately from the law of sines.

We find that Equations (4.31), (4.32), (4.33), and (4.34) have the corresponding equations: Equations (4.10), (4.11), (4.12), and (4.13) in Section *Parametrization of Catmull-Clark Subdivision Surfaces* (Sec. 4.1.4). Using the same methods as the previ-

ous section, we have the value of β_n:

$$\beta_n = \arcsin\left(\frac{bc + \sqrt{a^4 + a^2b^2 - a^2c^2}}{a^2 + b^2}\right). \tag{4.35}$$

where

$$\begin{aligned} \alpha_n &= \tfrac{\pi}{n} \\ a &= -3\sin(\alpha_n)\cos(\alpha_n) \\ b &= 4 + 3\cos^2(\alpha_n) \\ c &= \sin(\alpha_n) \end{aligned}$$

and $0 < \beta_n < \frac{\pi}{n}$; $k_n < 1$ when $n > 4$.

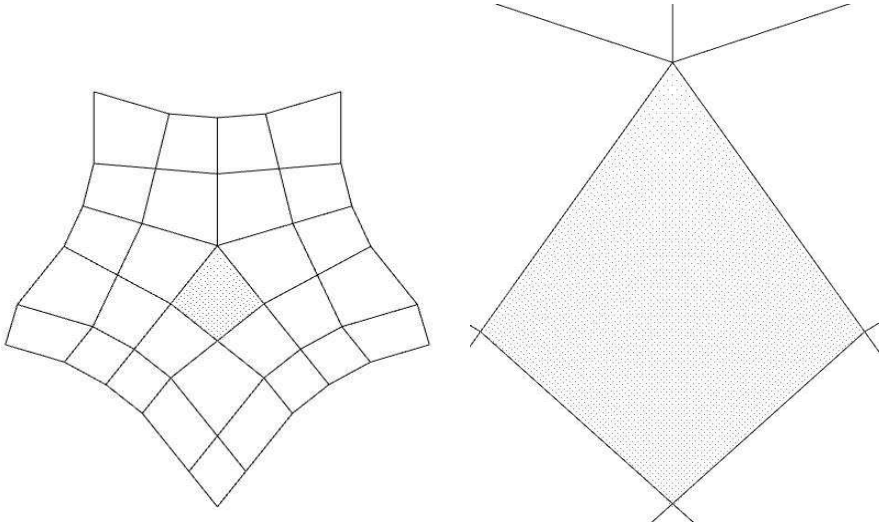

Figure 4.16: The domain (shaded area) of the 4-8 patch: $n = 5$.

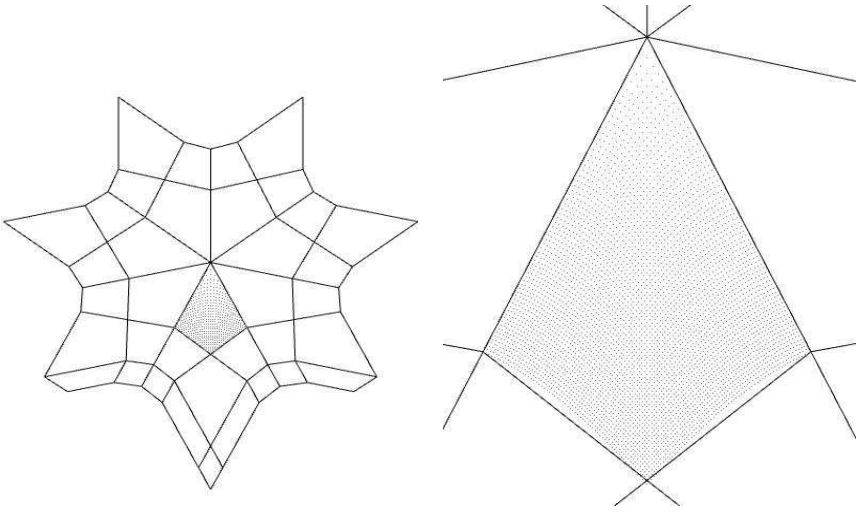

Figure 4.17: The domain (shaded area) of the 4-8 patch: $n = 7$.

Having the value of β_n, we can get the value of k_n and w_n. Now we can obtain the exact parametrization of 4-8 subdivision surfaces (cf. Figures 4.12 and 4.13).

The domain Ω_n of the 4-8 patch is the limit of the subdivision applied to the initial mesh of the abscissae v_i. We choose the abscissae mesh to be symmetric with respect to the extraordinary vertex. Then Ω_n falls into the sector formed by the initial abscissa quadrilateral with vertices v_0, v_1, v_2, and v_3 (see Figure 4.8). We find that the domains of the patches are strictly within the center quadrilaterals and the domains of the patches cover almost all the center quadrilaterals. Therefore, the bounds on subdivision surfaces are safe and efficient.

4.2.5 Computation of Exact Parametrization (Category II)

The parametrization of Category II is divided into two sub-categories:

1. The valence of the extraordinary vertex of the patch $n = 3$.
2. The valence of the extraordinary vertex of the patch $n > 4$.

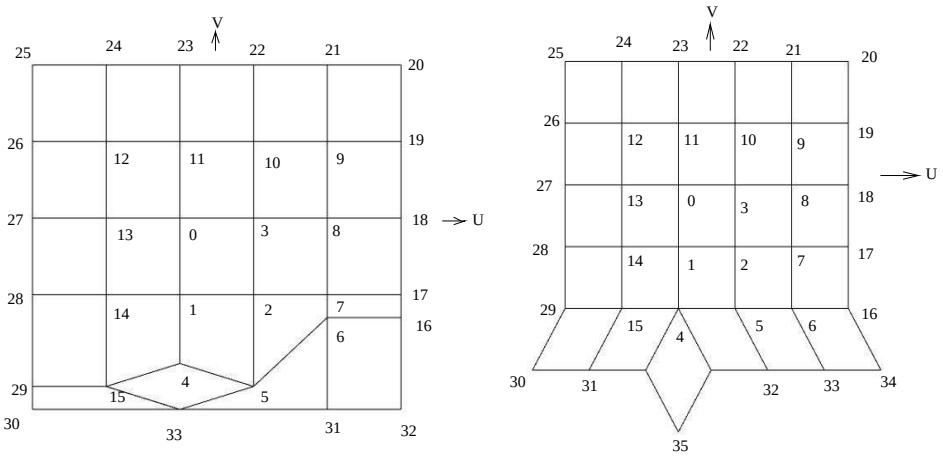

(a) n=3 (b) n=5

Figure 4.18: Parametrization of the 4-8 patches: Category II.

The construction of the parametrization of the first sub-category of category II is defined as follows:

1. Set $v_0 = 0$, the origin of the (u, v) plane.

2. The center quadrilateral is square, the length of each edge of the square is 1.
3. Let the edge v_0v_1 be situated on the v axis and the edge v_0v_3 situated on the u axis.
4. Extend the edge v_0v_1 by λ to get v_4. The value of λ is to be defined below.
5. Extend the edge v_3v_2 by ζ to get v_5. The value of ζ is to be defined below.
6. Extend the edges $v_1v_2, v_0v_3, v_2v_3, v_0v_1, v_0v_3$, and v_1v_2 by 1 to get $v_7, v_8, v_{10}, v_{11}, v_{13}$, and v_{14}.
7. Extend the edge v_7v_8 by γ to get v_6. The value of γ is to be defined below.
8. Extend the edges $v_7v_8, v_{10}v_{11}$ by 1 to get v_9, v_{12}.
9. Extend the edges $v_{13}v_{14}$ by ζ to get v_{15}.
10. Extend the edges $v_2v_7, v_3v_8, v_9v_{10}, v_8v_9, v_3v_{10}, v_0v_{11}, v_{12}v_{13}, v_{11}v_{12}, v_0v_{13}, v_0v_{14}$ by 1 to get $v_{17}, v_{18}, v_{19}, v_{21}, v_{22}, v_{23}, v_{24}, v_{26}, v_{27}, v_{28}$.
11. Extend the edges $v_{17}v_{18}$ by γ to get v_{16}.
12. Extend the edges $v_{18}v_{19}, v_{23}v_{24}$ by 1 to get v_{20}, v_{25}.
13. Extend the edges $v_{27}v_{28}$ by ζ to get v_{29}.
14. v_{33} defined by adding $v_5 - v_4$ to v_{15}.
15. Extend the edge $v_{28}v_{29}$ by the length between v_{15} and v_{33} in the v direction.
16. Extend the edge v_6v_7 by the length between v_6 and v_{33} in the v direction.
17. Extend the edge $v_{17}v_{16}$ by the length between v_{16} and v_{33} in the v direction.

We set $\lambda = 0.9$, $\gamma = 0.3$, and $\zeta = 1.2$. The choices of λ, γ, and ζ are made on intuitive grounds to ensure a well-formed mesh in the plane.

We know that to envelop a limit surface of this type, we need consider the vertices v_0, v_1, v_2 and v_3 and their one-ring neighbors. The limit positions of v_0 and v_3 are always equal to their original positions by the symmetry of their one-ring neighbors. We will also choose parameter values so that v_1 and v_2 are mapped into themselves by the subdivision process. Because v_1 and v_2 are regular vertices, we can compute their

limit positions by using the regular vertex limit position mask computed in the previous section:

$$\left(\frac{8}{28}, \frac{1}{28}, \frac{4}{28}, \frac{1}{28}, \frac{4}{28}, \frac{1}{28}, \frac{4}{28}, \frac{1}{28}, \frac{4}{28}\right).$$

To compute the limit position of v_1, we consider $v_0, v_2, v_3, v_4, v_5, v_{13}, v_{14}$, and v_{15}. In fact, just the vertical components of v_4, v_5, and v_{15} will affect the position of v_1. The vertical components (positive downwards) of v_5 and v_{15} are 2.2, which are 0.2 unit more than these of regular vertices. The vertical component (positive downwards) of v_4 is 1.9, which is 0.1 unit less than that of regular vertex. From the limit position mask, we know v_4 has four times the weights of v_{15} and v_5. The weights that affect the position of v_1 are

$$0.2 + 0.2 + 4 * (-0.1) = 0. \tag{4.36}$$

So the limit position of v_1 is equal to the original position.

To compute the limit position of v_2, we consider $v_0, v_1, v_3, v_4, v_5, v_6, v_7$, and v_8. In fact, just the vertical components (positive downwards) of v_4, v_5, and v_6 will affect the position of v_2. The vertical component of v_4 is 1.9, which is 0.1 less than that of regular case. The vertical component of v_5 is 2.2, which is 0.2 more than that of regular case. The vertical component of v_6 is 1.3, which is 0.7 less than that of regular case.

From the limit position mask, we know v_5 has four times the weights of v_4 and v_6. The weights that affect the position of v_2 are:

$$0.2 * 4 - 0.7 - 0.1 = 0. \tag{4.37}$$

So the limit position of v_2 is equal to the original position. We find that the domains of the patches with this parametrization are strictly within the center quadrilaterals and the domains are also close to the center quadrilaterals. Therefore, the bounds on subdivision surfaces are safe and efficient.

The construction of the parametrization of the second sub-category of category II is defined as follows:

1. Set $v_0 = 0$, the origin of (u, v) plane.
2. The center quadrilateral is square, the length of each edge of the square is 1.
3. Let the edge v_0v_1 be situated on the v axis and the edge v_0v_3 situated on the u axis.

4. Extend the edges v_0v_1, v_2v_3, v_1v_2, v_0v_3, v_2v_3, v_0v_1, v_0v_3, and v_1v_2 by 1 to get v_4, v_5, v_7, v_8, v_{10}, v_{11}, v_{13}, and v_{14}.

5. Extend the edges $v_4v_5, v_7v_8, v_{10}v_{11}$, and $v_{13}v_{14}$ by 1 to get v_6, v_9, v_{12}, and v_{15}.

6. Extend the edges $v_5v_6, v_2v_7, v_3v_8, v_9v_{10}, v_8v_9, v_3v_{10}, v_0v_{11}, v_{12}v_{13}, v_{11}v_{12}, v_0v_{13}, v_1v_{14}$, and v_4v_{15} by 1 to get $v_{16}, v_{17}, v_{18}, v_{19}, v_{21}, v_{22}, v_{23}, v_{24}, v_{26}, v_{27}, v_{28}$, and v_{29}.

7. From v_4 between the edge v_4v_{15} and v_4v_5 add $(n-3)$ edges in the counterclockwise direction. These edges from v_4v_{35} to v_4v_{32+n}. The angles between two consecutive edges are $\frac{\pi}{n-1}$ and the length of these edges is 1. After adding these edges, we get vertices from v_{35} to v_{32+n}.

8. From v_{15} and v_{29} add $v_{35} - v_4$ to get v_{31} and v_{30}.

9. From v_5, v_6, and v_{16} add $v_{32+n} - v_4$ to get v_{32}, v_{33}, and v_{34}.

As mentioned, the choice of the layout around the extraordinary vertex v_4 was made on intuitive grounds to ensure a well-formed mesh in the plane.

We find that the one-ring neighbors of each of the vertices of the center quadrilateral are symmetric. We are sure that the domain of this patch matches the center quadrilateral exactly.

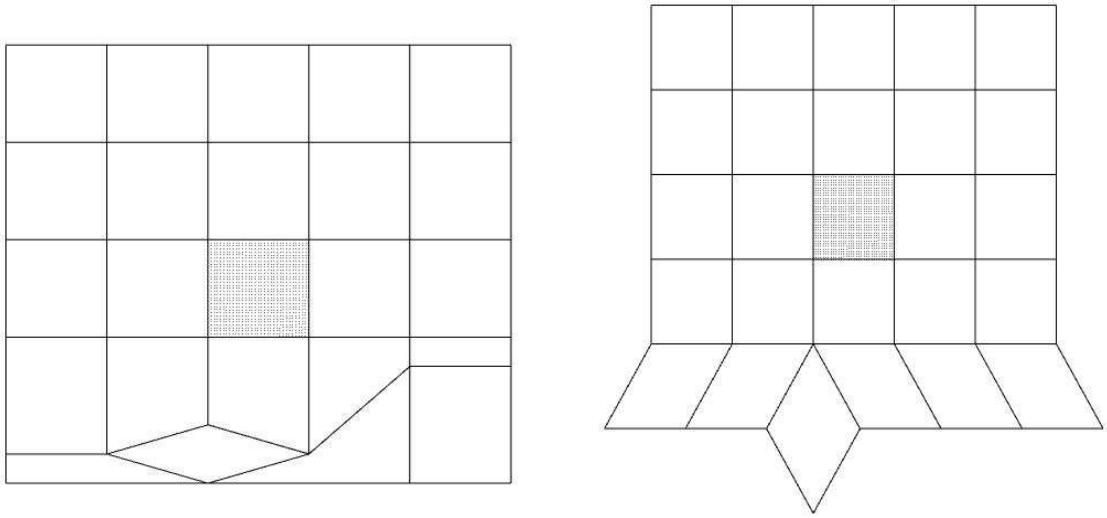

Figure 4.19: The domains (shaded areas) of the 4-8 patches (Category II).

4.2.6 Computation of Exact Parametrization (Category III)

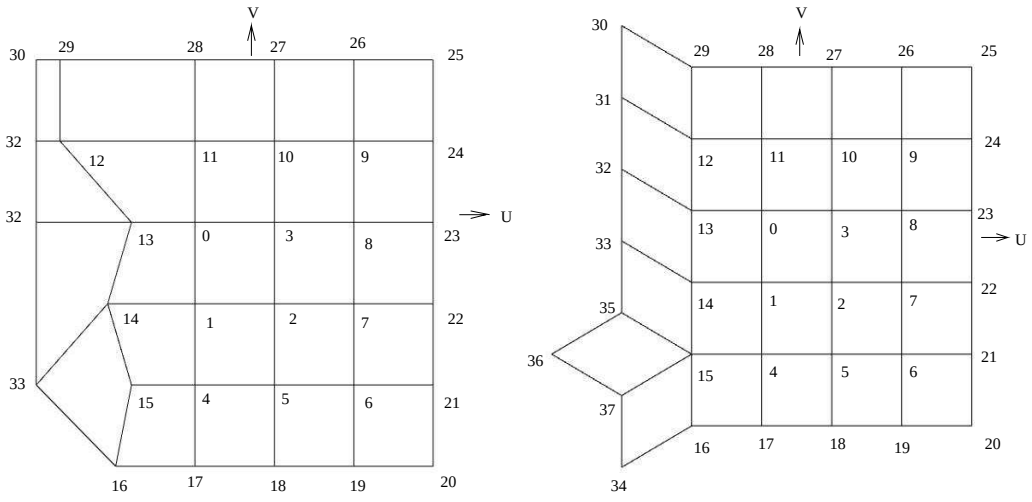

(a) n=3 (b) n=5

Figure 4.20: Parametrization of the 4-8 patches: Category III.

The parametrization of Category III is divided into two sub-categories:

1. The valence of the extraordinary vertex of the patch $n = 3$.

2. The valence of the extraordinary vertex of the patch $n > 4$.

The construction of the parametrization of the first sub-category of category III is defined as follows:

1. Set $v_0 = 0$, the origin of the (u, v) plane.
2. The center quadrilateral is square, the length of each edge of the square is 1.
3. Let the edge v_0v_1 be situated on the v axis and the edge v_0v_3 situated on the u axis.
4. Extend the edges $v_0v_1, v_2v_3, v_1v_2, v_0v_3, v_2v_3$, and v_0v_1 by 1 to get $v_4, v_5, v_7, v_8, v_{10}$, and v_{11}.
5. Extend the edge v_0v_3 by σ to get v_{13}. The value of σ is to be defined below.
6. Extend the edge v_1v_2 by ω to get v_{14}. The value of ω is to be defined below.
7. Extend the edges v_4v_5 and v_7v_8 by 1 to get v_6 and v_9.
8. Extend the edge $v_{10}v_{11}$ by φ to get v_{12}. The value of φ is to be defined below.
9. Extend the edge v_4v_5 by σ to get v_{15}.
10. Extend the edges $v_1v_4, v_2v_5, v_6v_7, v_5v_6, v_2v_7, v_3v_8, v_9v_{10}, v_8v_9, v3v_{10}$, and v_0v_{11} by 1. to get $v_{17}, v_{18}, v_{19}, v_{21}, v_{22}, v_{23}, v_{24}, v_{26}, v_{27}$, and v_{28}.
11. Extend the edges $v_{17}v_{18}, v_{18}v_{19}$, and $v_{24}v_{25}$ by 1.0 to get v_{16}, v_{20}, and v_{25}.
12. Extend the edge $v_{27}v_{28}$ by φ to get v_{29}.
13. Extend the edges $v_{27}v_{28}, v_{10}v_{11}, v_0v_3$, and v_4v_5 by 2.0 to get v_{30}, v_{31}, v_{32}, and v_{33}.

We set $\sigma = 0.8$, $\omega = 1.1$, and $\varphi = 1.7$. The choices of σ, ω, and φ on the intuitive grounds to ensure a well-formed mesh in the plane.

We know that to envelop a limit surface of this type, we need consider the positions of v_0, v_1, v_2, v_3 and their one-ring neighbors. The limit positions of v_2 and v_3 are always equal to their original positions by the symmetry of their one-ring neighbors. We will also choose parameter values so that v_0 and v_1 are mapped into themselves. Because v_0

and v_1 are regular vertices, we can compute their limit positions by using the regular vertex limit position mask computed in the previous section:

$$\left(\frac{8}{28}, \frac{1}{28}, \frac{4}{28}, \frac{1}{28}, \frac{4}{28}, \frac{1}{28}, \frac{4}{28}, \frac{1}{28}, \frac{4}{28}\right).$$

To compute the limit position of v_0, we consider $v_1, v_2, v_3, v_{10}, v_{11}, v_{12}, v_{13}$, and v_{14}. In fact, the horizontal components of these vertices affect the position of v_0. We just need adjust positions of v_{12}, v_{13}, and v_{14}. The horizontal component (positive leftwards) of v_{12} is 2.7, which is 0.7 unit more than that of regular case. The horizontal component (positive leftwards) of v_{13} is 1.8, which is 0.2 less than that of regular case. The horizontal component (positive leftwards) of v_{14} is 2.1, which is 0.1 unit more than that of regular case. From the limit position mask, we know v_{13} has four times the weights of v_{12} and v_{14}. The weights that affect the position of v_0 are:

$$-0.2 * 4 + 0.1 + 0.7 = 0. \tag{4.38}$$

So the limit position of v_0 is equal to its original position.

To compute the limit position of v_1, we consider the vertices of $v_0, v_2, v_3, v_4, v_5, v_{13}, v_{14}$, and v_{15}. In fact, just the horizontal components of these vertices affect the position of v_1. We just need adjust positions of v_{13}, v_{14}, and v_{15}. The horizontal component (positive leftwards) of v_{13} is 1.8, which is 0.2 unit less than that of regular case. The horizontal component (positive leftwards) of v_{14} is 2.1, which is 0.1 unit more than that of regular case. The horizontal component (positive leftwards) of v_{15} is 1.8, which is 0.2 unit less than that of regular case. From the limit position mask, we know v_{14} has four times the weights of v_{13} and v_{15}. The weights that affect the position of v_1 are:

$$0.1 * 0.4 - 0.2 - 0.2 = 0. \tag{4.39}$$

So the limit position of v_2 is equal to its original position.

We find that the domains of the patches with this parametrization are strictly within the center quadrilaterals and the domains are also close to the center quadrilaterals. Therefore, the bounds on subdivision surfaces are safe and efficient.

The construction of the parametrization of the second sub-category of category III is defined as follows:

1. Set $v_0 = 0$, the origin of (u, v) plane.

2. The central quadrilateral is square, the length of each edge of the square is 1.

3. Let the edge v_0v_1 be situated on the v axis and the edge v_0v_3 situated on the u axis.

4. Extend the edges $v_0v_1, v_2v_3, v_1v_2, v_0v_3, v_2v_3, v_0v_1, v_0v_3,$ and v_1v_2 by 1.0 to get $v_4, v_5, v_7, v_8, v_{10}, v_{11}, v_{13},$ and v_{14}.

5. Extend the edges $v_4v_5, v_7v_8, v_{10}v_{11},$ and $v_{13}v_{14}$ by 1.0 to get $v_6, v_9, v_{12},$ and v_{15}.

6. Extend the edges $v_1v_4, v_2v_5, v_6v_7, v_5v_6, v_2v_7, v_3v_8, v_9v_{10}, v_8v_9, v_3v_{10},$ and v_0v_{11} by 1.0 to get $v_{17}, v_{18}, v_{19}, v_{21}, v_{22}, v_{23}, v_{24}, v_{26}, v_{27}$ and v_{28}.

7. Extend the edges $v_{14}v_{15}, v_{18}v_{19}, v_{24}v_{25},$ and $v_{27}v_{28}$ by 1.0 to get $v_{16}, v_{20}, v_{25},$ and v_{29}.

8. Add $(n-3)$ edges incident at v_{15} between the edge $v_{15}v_{14}$ and the edge $v_{15}v_{16}$ in the direction counterclockwise. The angles between two consecutive edges are $\frac{\pi}{(n-1)}$ and the length of these edges is 1.0. After adding these edges, we get vertices from v_{35} to v_{32+n}.

9. From $v_{29}, v_{12}, v_{13},$ and v_{14} add $(v_{35} - v_{15})$ to get $v_{30}, v_{31}, v_{32},$ and v_{33}.

10. From v_{16} add $v_{37} - v_{15}$ to get v_{34}.

As mentioned, the choice of the layout around the extraordinary vertex v_{15} was made on intuitive grounds to ensure a well-formed mesh in the plane.

We find that the one-ring neighbors of each of the vertices of the center quadrilateral are symmetric. We are sure that the domain of this patch matches the center quadrilateral exactly.

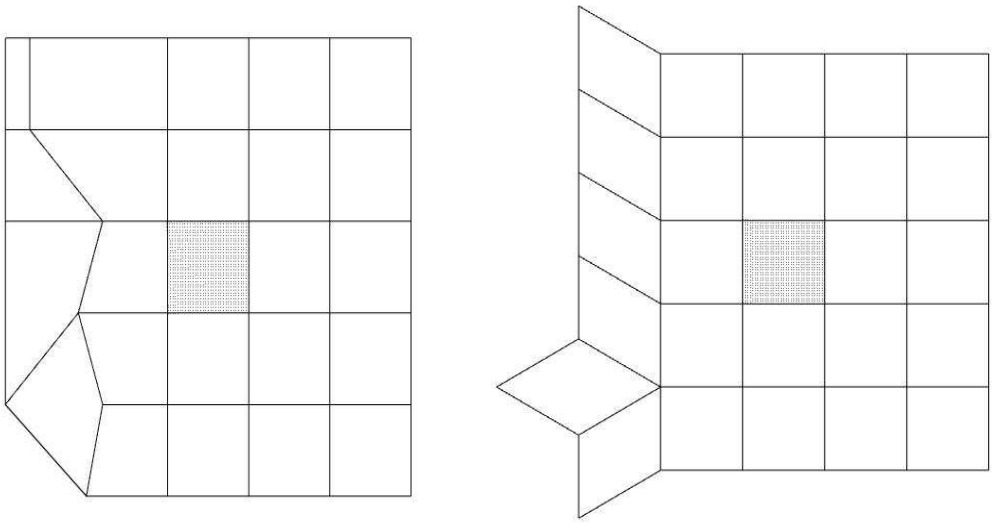

Figure 4.21: The domains (shaded areas) of the 4-8 patches (Category III).

4.2.7 Computation of Exact Parametrization (Category IV)

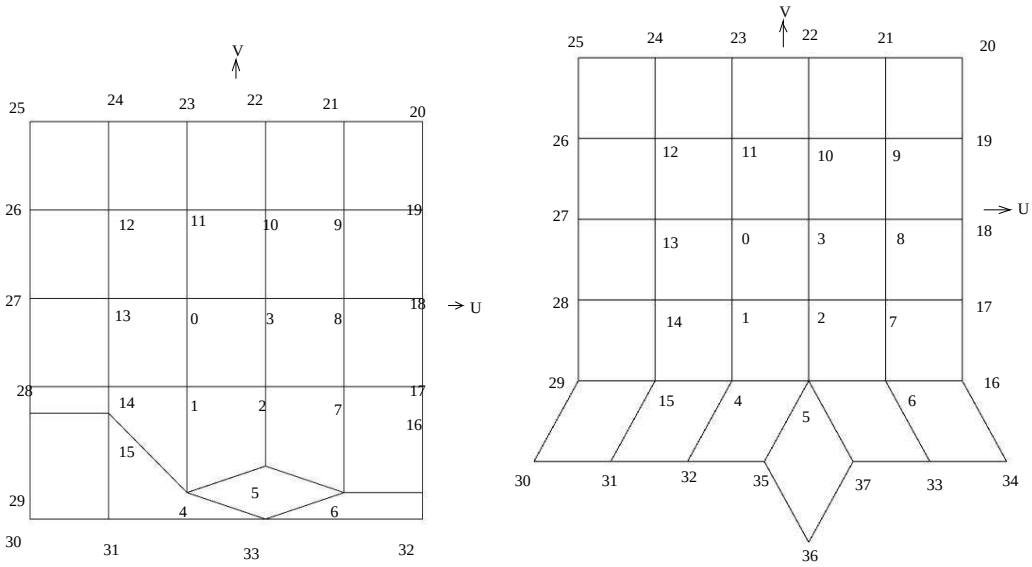

(a) n=3 (b) n=5

Figure 4.22: Parametrization of the 4-8 patches: Category IV.

The parametrization of Category IV is divided into two sub-categories:

1. The valence of the extraordinary vertex of the patch $n = 3$.

2. The valence of the extraordinary vertex of the patch $n > 4$.

The construction of the parametrization of the first sub-category of category IV is defined as follows:

1. Set $v_0 = 0$, the origin of the (u, v) plane.
2. The central quadrilateral is square, the length of each edge of the square is 1.
3. Let the edge v_0v_1 be situated on the v axis and the edge v_0v_3 situated on the u axis.
4. Extend the edge v_0v_1 by κ to get v_4. The value of κ is to be defined below.
5. Extend the edge v_2v_3 by ξ to get v_5. The value of ξ is to be defined below.
6. Extend the edges $v_1v_2, v_0v_3, v_2v_3, v_0v_1, v_0v_3$, and v_1v_2 by 1.0 to get $v_7, v_8, v_{10}, v_{11}, v_{13}$, and v_{14}.
7. Extend the edge v_7v_8 by κ to get v_6.
8. Extend the edges v_7v_8 and $v_{10}v_{11}$ by 1.0 to get v_9 and v_{12}.
9. Extend the edge $v_{13}v_{14}$ by ϱ to get v_{15}. The value of ϱ is to be defined below.
10. Extend the edges $v_2v_7, v_3v_8, v_9v_{10}, v_8v_9, v_3v_{10}, v_0v_{11}, v_{12}v_{13}, v_{11}v_{12}, v_0v_{13}$, and v_1v_{14} by 1.0 to get $v_{17}, v_{18}, v_{19}, v_{21}, v_{22}, v_{23}, v_{24}, v_{26}, v_{27}$, and v_{28}.
11. Extend the edge $v_{17}v_{18}$ by κ to get v_{16}.
12. Extend the edges $v_{18}v_{19}$, and $v_{23}v_{24}$ by 1.0 to get v_{20}, and v_{25}.
13. Extend the edge $v_{27}v_{28}$ by ϱ to get v_{29}.
14. Extend the edges $v_{27}v_{28}, v_{13}v_{14}, v_2v_3$, and $v_{17}v_{18}$ by 2.0 to get v_{30}, v_{31}, v_{33}, and v_{32}.

We set $\kappa = 1.2, \xi = 0.9$, and $\varrho = 0.3$. The choices of κ, ξ, and ϱ are made on intuitive grounds to ensure a well-formed mesh in the plane.

We know to envelop the limit surface of this type, we need consider the vertices v_0, v_1, v_2, v_3 and their one-ring neighbors. The limit positions of v_0 and v_3 are always equal to their original positions by the symmetry of their one-ring neighbors. We will also choose parameter values so that v_1 and v_2 are mapped into themselves. Because v_1

and v_2 are regular vertices, we can compute their limit positions by using the regular vertex limit position mask computed in the previous section:

$$\left(\frac{8}{28}, \frac{1}{28}, \frac{4}{28}, \frac{1}{28}, \frac{4}{28}, \frac{1}{28}, \frac{4}{28}, \frac{1}{28}, \frac{4}{28}\right).$$

To compute the limit position of v_1, we consider $v_0, v_2, v_3, v_4, v_5, v_{13}, v_{14}$, and v_{15}. In fact, the vertical components of these vertices affect the position of v_1. We just need adjust the positions of v_4, v_5, and v_{15}. The vertical component (positive downwards) of v_{15} is 1.3, which is 0.7 unit less than that in regular patch. The vertical component (positive downwards) of v_4 is 2.2, which is 0.2 unit more than that in regular case. The vertical component (positive downwards) of v_5 is 1.9, which is 0.1 unit less than that of regular case. From the limit position mask, we know v_4 has four times the weights of v_{15} and v_5. The weights that affect the position v_1 are:

$$-0.2 * 4 + 0.7 + 0.1 = 0.$$

So the limit position of v_1 is equal to its original position.

To compute the limit position of v_2, we consider $v_0, v_1, v_3, v_4, v_5, v_6, v_7$, and v_8. In fact, the vertical components of these vertices affect the position of v_2. We just need adjust the positions of v_4, v_5, and v_6. The vertical component (positive downwards) of v_4 is 2.2, which is 0.2 unit more than that of regular case. The vertical component (positive downwards) of v_5 is 1.9, which is 0.1 unit less than that of regular case. The vertical component (positive downwards) of v_6 is 2.2, which is 0.2 unit more than that of regular case. From the limit position mask, we know v_5 has four times the weights of v_4 and v_6. The weights that affect the position of v_2 are:

$$-0.1 * 4 + 0.2 + 0.2 = 0.$$

So the limit position of v_1 is equal to its original position.

We find that the domains of the patches with this parametrization are strictly within the center quadrilaterals and the domains are also close to the center quadrilaterals. Therefore, the bounds on subdivision surfaces are safe and efficient.

The construction of the parametrization of the second sub-category of category IV is defined as follows:

1. Set $v_0 = 0$, the origin of (u, v) plane.

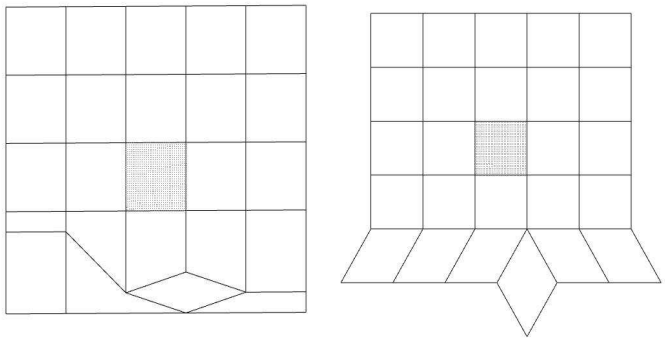

Figure 4.23: The domains (shaded areas) of the 4-8 patches (Category IV).

2. The central quadrilateral is square, the length of the square is 1.

3. Let the edge v_0v_1 be situated on the v axis and the edge v_0v_3 situated on the u axis.

4. Extend the edges $v_0v_1, v_2v_3, v_1v_2, v_0v_3, v_2v_3, v_0v_1, v_0v_3$, and v_1v_2 by 1.0 to get $v_4, v_5, v_7, v_8, v_{10}, v_{11}, v_{13}$, and v_{14}.

5. Extend the edges $v_4v_5, v_7v_8, v_{10}v_{11}$, and $v_{13}v_{14}$ by 1.0 to get v_6, v_9, v_{12}, and v_{15}.

6. Extend the edges $v_5v_6, v_2v_7, v_3v_8, v_9v_{10}, v_8v_9, v_3v_{10}, v_0v_{11}, v_{11}v_{12}, v_0v_{13}, v_1v_{14}$, and v_4v_{15} by 1.0 to get $v_{16}, v_{17}, v_{18}, v_{19}, v_{21}, v_{22}, v_{23}, v_{24}, v_{26}, v_{27}, v_{28}$, and v_{29}.

7. Add (n - 3) edges incident at v_5 between the edge v_5v_4 and the edge v_5v_6 in the direction counterclockwise. The angle between two consecutive edges is $\frac{\pi}{(n-2)}$ and the length of these edges is 1.0. After adding these edges, we get vertices v_{35+2i}. $(i = 0, ..., n-4)$.

8. Add $v_5 - v_{35+(2m+2)}$ to the vertices v_{35+2m} to get $v_{35+(2m+1)}$. $(i = 0, ..., n-5)$.

Again as mentioned, the choice of the layout around the extraordinary vertex v_5 was made on intuitive grounds to ensure a well-formed mesh in the plane.

We find that the one-ring neighbors of each of the vertices of the center quadrilateral are symmetric. Yet again, we are sure that the domain of this patch matches center quadrilateral exactly.

Chapter 5

Conclusion and Future Work

This chapter summarizes the thesis, reviews its contributions and proposes directions for future work.

5.1 Summary

In this thesis, we presented our work on the parametrization of Catmull-Clark and 4-8 subdivision surfaces. The parametrization of Catmull-Clark subdivision surfaces is based on a set of Catmull-Clark patches and the parametrization of 4-8 subdivision surfaces is based on a set of 4-8 patches. Therefore, the main part of this thesis is to define parametric domains for the Catmull-Clark and 4-8 patches which permit guaranteed but realistic bounds on the patches themselves. The principle is to assure the domain of one patch is strictly within the center quadrilateral of the patch. In addition, we ensured that the vertices of the center quadrilateral of the patch are mapped to themselves by the subdivision process. This is to be done by choosing carefully the parameter values of the patch. This produced domains which matched the enclosing quadrilaterals closely.

We showed experimentally that the domains of the Catmull-Clark and 4-8 patches with valence up to 25 are strictly within the center quadrilaterals. This fact is important so that we can envelop the limit surfaces of the Catmull-Clark and 4-8 subdivision surfaces with our method of parametrization.

5.2 Future Work

A possible extension to the current work is a theoretic justification for the parametrization of the subdivision surfaces. In our thesis, we showed how to choose the parameter values of the patch to map the vertices of the center quadrilateral of the patch to themselves by the subdivision process. It is true that the domain of the patch is strictly within the center quadrilateral only if the domain bulges inward. We have only shown experimentally that the domain of the patch ($n > 4$) bulges inward.

Another possible extension to the current work is to reduce as much as possible the difference between the domain of the patch and the center quadrilateral by modifying the parameter values of the patch. This would improve computational precision in the various applications such as measuring the maximum error between the subdivision surface and its linear approximation. We have not examined the effects in model space of the parametric domains we have found.

An analysis of the empirical convergence of the subdivision surfaces of Catmull-Clark and 4-8 subdivision is also an interesting subject. We can analyze these two kinds of subdivision surfaces by measuring the flatness of the limit surface, or the maximum bounding error between the subdivision surface and its linear approximation.

In our thesis, we showed how to parametrize the Catmull-Clark and 4-8 subdivision surfaces. We can apply these parametrizations to many interesting domains, such as interference detection and ray-tracing of the Catmull-Clark and 4-8 subdivision surfaces.

Bibliography

[1] ACIS. The ACIS 3D Toolkit Guide. *Spatical Technology*, 1999.

[2] L.-E. Andersson and N. F. Stewart. *An Introduction to the Mathematics of Subdivision Surfaces*. SIAM, 2010.

[3] L.-E. Andersson, N. F. Stewart, and M. Zidani. Error analysis for operations in solid modeling in the presence of uncertainty. *SIAM Journal on Scientific Computing*, pages 811–826, 2007.

[4] A. A. Ball and D. J. T. Storry. A matrix approach to the analysis of recursively generated B-spline surface. *Computer Aided Design*, pages 437–442, 1986.

[5] P. Bamberg and S. Sternberg. *A course in Mathematics for Students of Physics*. Cambridge University Press, 1991.

[6] W. Böhm, G. Farin, and J. Kahmann. A survey of curve and surface methods in CAGD. *Computer Aided Geometric Design*, pages 1–60, 1984.

[7] E. Catmull and J. Clark. Recursively generated B-spline surfaces on aribitrary topological meshes. *Computer Aided Design*, pages 350–355, 1978.

[8] G. M. Chaikin. An algorithm for high speed curve generation. *Computer Graphics and Image Processing*, pages 346–319, 1974.

[9] G. De Rham. Sur une courbe plane. *J. de Mathématiques Pures et Appliquées*, pages 25–42, 1956.

[10] T. DeRose, M. Kass, and T. Truong. Subdivision surfaces in character animation. *In Proceedings of SIGGRAPH '98*, pages 85–94, 1998.

[11] D. Doo and M. Sabin. Behaviour of recursive sudivision surfaces near extraordinary points. *Computer-Aided Design*, pages 356–360, 1978.

[12] B. Grünbaum and G. C. Shephard. *Tilings and Patterns*. W.H. Freeman, 1987.

[13] M. Halstead, M. Kass, and T. DeRose. Efficient, fair interpolation using Catmull-Clark Surfaces. *In Proceedings of SIGGRAPH '93*, pages 34–44, 1993.

[14] C. M. Hoffmann. *Geometric and solid modeling: an introduction*. Morgan Kaufmann Publishers, Inc., 1989.

[15] D. Jiang. *Reliable Computation for Geometric Models*. PhD thesis, Department of informatique and recherche opérationnelle, University of Montreal, 2009.

[16] P. Jörg and U. Reif. *Subdivision Surfaces*. Springer, 2008.

[17] L. Kobbelt. Tight Bounding Volumes for Subdivision Surfaces. *In Proceedings of Pacific Graphics '98*, pages 17–26, 1998.

[18] C. T. Loop. Smooth subdivision surfaces based on triangles. Master's thesis, Department of Mathematics,University of Utah, 1987.

[19] J. R. Shewchuk. Mesh generation for domains with small angles. *In Proceedings of the Sixteenth Annual ACM Symposium Computational Geometry*, pages 1–10, 2000.

[20] J. Stam. Evaluation of Loop Subdivision Surfaces. *In Proceedings of SIGGRAPH '98*, 1998.

[21] J. Stam. Exact Evaluation of Catmull-Clark Subdivision Surfaces at Arbitrary Parameter Values. *In Proceedings of SIGGRAPH '98*, pages 395–404, 1998.

[22] J. Stam. On subdivision schemes generalizing uniform B-spline surfaces of high degree. *Computer Aided Geometric Design*, pages 383–396, 2001.

[23] L. Velho and D. Zorin. 4-8 Subdivision. *Computer Aided Geometric Design*, pages 397–427, 2001.

[24] X. Wu and J. Peters. Interference Detection for Subdivision surfaces. *In Proceedings of Eurographics '04*, pages 577–585, 2004.

[25] X. Wu and J. Peters. An Accurate Error Measure for Adaptive Subdivision Surfaces. *In Proceedings of the International Convention on Shapes and Solids SMI-05*, pages 51–57, 2005.

[26] D. Zorin and P. Schröder. Subdivision for Modeling and Animation. In *ACM SIGGRAPH '00 Course Notes*, 2000.

[27] D. Zorin and P. Schröder. A unified framework for primal/dual quadrilateral subdivision schemes. *Computer Aided Geometric Design*, pages 429–454, 2001.